General Disclaimer

One or more of the Following Statements may affect this Document

- This document has been reproduced from the best copy furnished by the organizational source. It is being released in the interest of making available as much information as possible.

- This document may contain data, which exceeds the sheet parameters. It was furnished in this condition by the organizational source and is the best copy available.

- This document may contain tone-on-tone or color graphs, charts and/or pictures, which have been reproduced in black and white.

- This document is paginated as submitted by the original source.

- Portions of this document are not fully legible due to the historical nature of some of the material. However, it is the best reproduction available from the original submission.

52

COO-1574-19

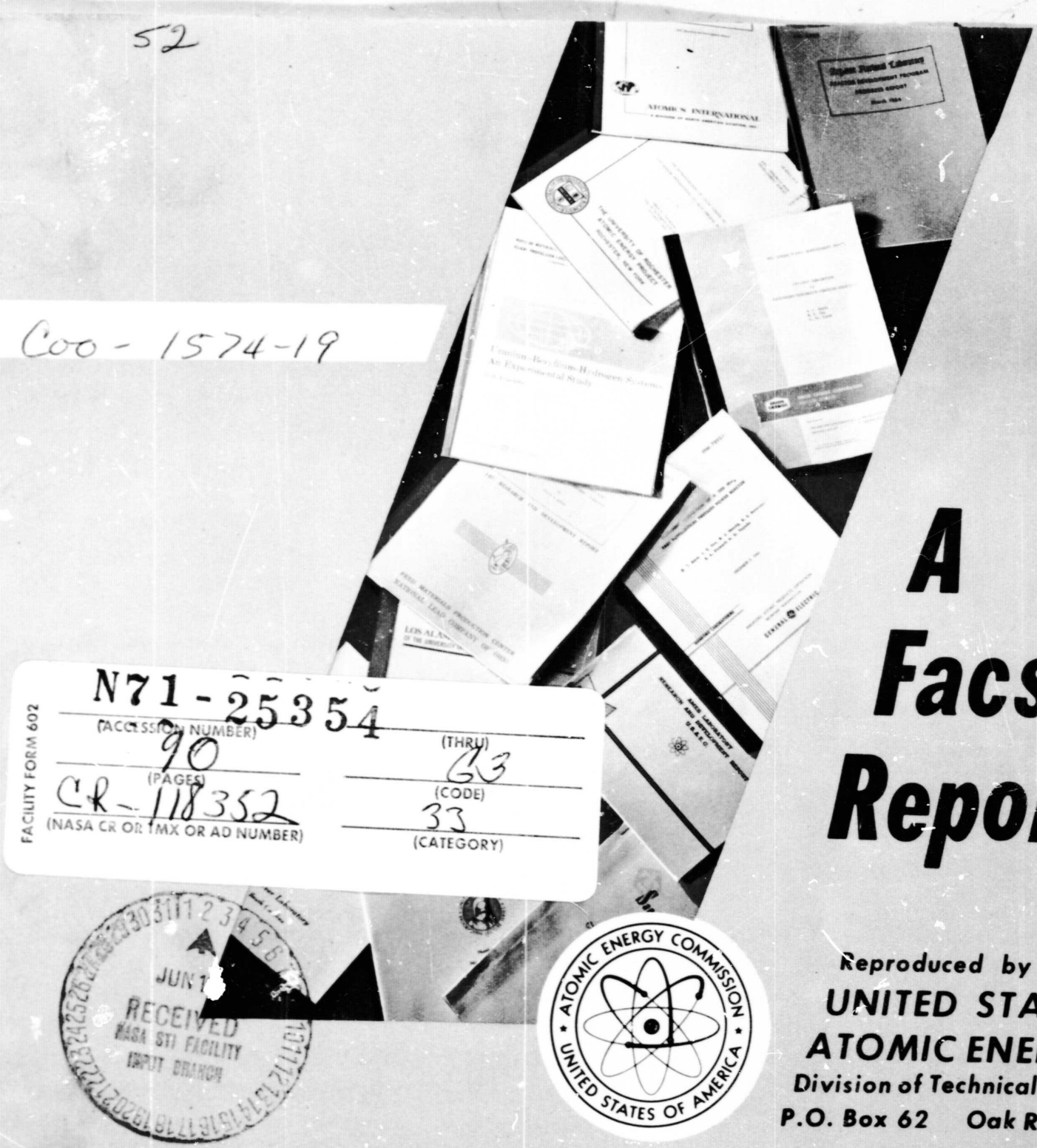

A

Facsimile Report

Reproduced by
UNITED STATES
ATOMIC ENERGY COMMISSION
Division of Technical Information
P.O. Box 62 Oak Ridge, Tennessee 37830

Dot-1505XR

COO-1574-19

MASTER

COUPLING BETWEEN PRESSURE AND TEMPERATURE WAVES IN LIQUID HELIUM

By

Garold F. Fritz

A THESIS

Submitted to

Michigan State University

in partial fulfillment of the requirements

for the degree of

DOCTOR OF PHILOSOPHY

Department of Physics

1970

ABSTRACT

COUPLING BETWEEN PRESSURE AND TEMPERATURE

WAVES IN LIQUID HELIUM

By

Garold F. Fritz

When the thermal expansion coefficient α is retained in the linearized hydrodynamic equations of the two-fluid model of superfluid liquid helium, pressure and temperature waves are not independent. Thus a periodically varying temperature source produces not only temperature waves in liquid helium, but also two pressure waves, p_1' and p_2', which propagate at the velocity of first and second sound, respectively. Similarly a vibrating diaphragm produces not only pressure waves but also two temperature waves, T_1' and T_2', which also propagate at the velocity of first and second sound, respectively. Lifshitz has shown that the amplitudes of these cross-modes should be proportional to α. This thesis is an investigation of this coupling by observing and studying the two pressure waves p_1' and p_2' produced by a heater and the temperature wave T_2' produced by a capacitor microphone. The temperature dependence of the amplitude of these waves has been studied using both pulse and standing wave techniques in the temperature range from 1.2 K to the λ-point. Good agreement with theory has resulted only for the p_1' mode.

COUPLING BETWEEN PRESSURE AND TEMPERATURE

WAVES IN LIQUID HELIUM

By

Garold F. Fritz

A THESIS

Submitted to

Michigan State University

in partial fulfillment of the requirements

for the degree of

DOCTOR OF PHILOSOPHY

Department of Physics

1970

To Carol

ACKNOWLEDGEMENTS

This experiment was suggested by Professor G. L. Pollack. I would like to thank him for his guidance and encouragement during the course of my work and for his advice in the preparation of this thesis. I would also like to express my gratitude to Dr. T. H. Edwards for the use of his vacuum coating equipment and to Mr. Carl James Duthler and Mr. Charles W. Leming for their assistance in the laboratory. Also, I wish to thank my wife, Carol, for typing the manuscript. I am also indebted to the U. S. National Aeronautics and Space Administration for support in the form of a three year fellowship. Finally I would like to acknowledge the financial support of the U. S. Atomic Energy Commission.

TABLE OF CONTENTS

LIST OF FIGURES

I. INTRODUCTION

Liquid ^{4}He cooled below 2.17 K, which is called the lambda temperature, exhibits a number of peculiar properties which have been successfully explained by the introduction of a two-fluid model.[1,2,3] In this model it is assumed that the ordered motion of the elementary excitations in the liquid is associated with only part of the liquid. This part is called the normal component and is characterized by the normal density ρ_n. The normal component has viscosity and its flow is described by a velocity field v_n. The remaining part of the liquid, which is called the superfluid component, is characterized by the density $\rho_s = \rho - \rho_n$, where ρ is the total density of the liquid. The superfluid component has no viscosity and performs an independent motion which is described by the velocity field v_s. No explicit assumptions are made about the temperature dependence of ρ_s and ρ_n except the following:

$$\frac{\rho_s}{\rho} = 0 \qquad \frac{\rho_n}{\rho} = 1 \qquad \text{at } T = T_\lambda = 2.17 \text{ K}$$

$$\frac{\rho_s}{\rho} = 1 \qquad \frac{\rho_n}{\rho} = 0 \qquad \text{at } T = 0.$$

With these assumptions a complete set of hydrodynamic equations can be derived for superfluid liquid helium.[4,5] One consequence of these hydrodynamic equations is the existence of two wave modes which propagate with different velocities. One of these wave modes is ordinary sound or pressure variations which propagate with the velocity $u_1 = \left[(\partial p/\partial \rho)_S\right]^{\frac{1}{2}}$, where p is the pressure and S the specific entropy. In the other wave mode the temperature is the fluctuating thermodynamic quantity. This mode is called "second sound". The velocity of second sound is $u_2 = \left[(TS^2/C)(\rho_s/\rho_n)\right]^{\frac{1}{2}}$, where C is the specific heat. The velocity u_2 is an order of magnitude lower than u_1 and vanishes at $T = T_\lambda$.

When terms containing the thermal expansion coefficient ($\alpha \equiv -(1/\rho)(\partial\rho/\partial T)$) are neglected, first and second sound are independent. In this approximation a vibrating diaphragm would produce only pressure waves which propagate at u_1; that is, pure first sound. Similarly a fluctuating temperature source would produce only temperature waves which propagate at u_2; that is, pure second sound.

When thermal expansion is taken into account pressure and temperature waves in liquid helium are coupled. In this case there exists both pressure and temperature fluctuations which propagate with each velocity u_1 and u_2.

The original theoretical treatment of this coupling is due to Lifshitz.[6] He has shown that the relative amplitudes of the pressure and temperature waves produced in liquid helium depend upon the boundary conditions at the transmitter.

The object of this experiment was to investigate this coupling by observing and studying the pressure waves produced in liquid helium by a fluctuating temperature source and the temperature waves produced by a vibrating diaphragm. The amplitudes of the two pressure waves produced by a fluctuating temperature source are denoted by p_1' and p_2'. The subscripts 1 or 2 indicate that the wave propagates at u_1 or u_2, respectively. Similarly the two temperature waves produced by a vibrating diaphragm are denoted by T_1' and T_2'.

The pressure waves produced in liquid helium by a periodically heated resistor have been studied by other investigators. Jacucci and Signorelli[7] have optically observed p_2' by the Debye-Sears effect. Eynatten, et al.[8] have also observed this wave mode with a magnetic microphone. Hofmann, et al.[9] have observed and studied both p_1' and p_2'. All of the above results agree neither with each other nor with the theoretical results calculated by Lifshitz.[6] The results of the independent measurements of this investigation are in substantial but not total agreement with those of Hofmann, et al.[9]

Historically the first attempt to observe second sound was made by Shalnikov and Sokolov who attempted to generate this wave with a piezoelectric crystal.[10] They were unsuccessful. This negative result was, in fact, the motivation for the above mentioned investigations by Lifshitz.[6] He showed that a much more effective method of producing second sound would be by periodic heating. When this was pointed

out second sound was soon observed[10] and has been comprehensively studied since that time.[1,2]

No successful attempts have been reported, since the work of Shalnikov and Sokolov, in which second sound produced by a vibrating mechanical transducer has been observed. In the present investigation second sound, produced by a capacitor microphone, has been observed. A new type of second sound receiver whose active element is a metalized porous diaphragm has been used to observe this wave mode.

II. THEORY

When dissipative terms are neglected, the complete set of hydrodynamic equations based on the two-fluid model of liquid helium can be determined from conditions imposed by the Galilean relativity principle and the necessary conservation laws.[5] The derivation is similar to that for an ordinary fluid except that an additional relation, which takes into account the superfluid properties, must be included. Most often this additional relation is an equation of motion for the superfluid component. This choice, however, is not unique.[11]

When dissipative processes are considered, additional terms must be included in all the hydrodynamic equations except the continuity equation. There is considerable disagreement among the various authors on the proper form of these terms.[2] For the purpose of studying first and second sound the hydrodynamic equations constructed by Landau and Khalatnikov[5] are the most useful.

In our investigation the amplitude of the sound waves is small enough that only terms linear in the normal fluid and superfluid velocities, v_n and v_s, need be retained. In this case the hydrodynamic equations due to Landau and Khalatnikov take the following form[5]:

$$\frac{\partial \rho}{\partial t} + \vec{\nabla}\cdot\vec{j} = 0 \tag{1}$$

$$\frac{\partial j_i}{\partial t} + \frac{\partial p}{\partial r_1} = \eta \frac{\partial}{\partial r_k}\left(\frac{\partial v_{n1}}{\partial r_k} + \frac{\partial v_{nk}}{\partial r_1} - \frac{2}{3}\delta_{1k}\frac{\partial v_{nl}}{\partial r_l}\right) + \frac{\partial}{\partial r_1}\left[\zeta_1 \vec{\nabla}\cdot(\vec{j} - \rho\vec{v}_n) + \zeta_2 \vec{\nabla}\cdot\vec{v}_n\right] \tag{2}$$

$$\frac{\partial \vec{v}_s}{\partial t} + \vec{\nabla}\mu = \vec{\nabla}\left[\zeta_3 \vec{\nabla}\cdot(\vec{j} - \rho\vec{v}_n) + \zeta_4 \vec{\nabla}\cdot\vec{v}_n\right] \tag{3}$$

$$\frac{\partial(\rho s)}{\partial t} + \rho s \vec{\nabla}\cdot\vec{v}_n = \frac{\kappa}{T}\nabla^2 T \tag{4}$$

In Eq. (2) summation over the repeated indices is implied. The various symbols in these equations are as follows:

$\vec{j}$ = mass flux = $\rho_s\vec{v}_s + \rho_n\vec{v}_n$ (5)

ρ = total liquid ^{4}He density = $\rho_s + \rho_n$ (6)

ρ_s = superfluid density

ρ_n = normal fluid density

v_s = superfluid velocity

v_n = normal fluid velocity

p = pressure

r_1 = i-th component of the position vector

S = specific entropy

μ = free entropy

T = temperature

κ = thermal conductivity coefficient

η = ordinary viscosity of the normal fluid

$\zeta_1, \zeta_2, \zeta_3, \zeta_4$ = coefficients of second viscosity

Equation 1 is, of course, the continuity equation representing conservation of mass. Equation 2 is the equation of motion of the fluid as a whole. Equation 3 is the equation of motion of the superfluid component. Finally Eq. 4 represents the balance of entropy. The coefficients of second viscosity represent energy losses associated with changes in density which occur rapidly in comparison with the relaxation time required for restoration of thermodynamic equilibrium.

If all dissipative terms are neglected and use is made of the thermodynamic relation[12]:

$$d\mu = -SdT + \frac{1}{\rho}dp \qquad (7)$$

then Eqs. (1) - (4) take the following form:

$$\frac{\partial \rho}{\partial t} + \vec{\nabla}\cdot\vec{j} = 0 \qquad (8)$$

$$\frac{\partial \vec{j}}{\partial t} + \vec{\nabla} p = 0 \qquad (9)$$

$$\frac{\partial \vec{v}_s}{\partial t} - S\vec{\nabla}T + \frac{1}{\rho}\vec{\nabla}p = 0 \qquad (10)$$

$$\frac{\partial (\rho S)}{\partial t} + \rho S \vec{\nabla}\cdot\vec{v}_n = 0 \qquad (11)$$

A. First and Second Sound

Plane wave solutions in which all quantities are proportional to $\exp\left[i\omega(t-x/u)\right]$, will now be considered. If the symbols ρ', p', T', and S' represent the variation of ρ, p, T, and S from their equilibrium values, Eqs. 8 - 11 become:

$$u\rho' - (\rho_s v_s + \rho_n v_n) = 0 \qquad (8a)$$

$$u(\rho_s v_s + \rho_n v_n) - p' = 0 \qquad (9a)$$

$$u\rho v_s + S\rho T' - p' = 0 \qquad (10a)$$

$$u(S\rho' + \rho S') - S\rho v_n = 0 \qquad (11a)$$

It has been assumed that the fluid is stationary at equilibrium so that v_n and v_s were not denoted with primes. In obtaining Eqs. 8a - 11a the expression for j in Eq. 5 has also been used. Eliminating $j = \rho_s v_s + \rho_n v_n$ from Eqs. 8a and 9a yields

$$u^2\rho' - p' = 0 \qquad (12)$$

Solving Eq. 11a for S' and then substituting expressions for ρ and ρ' obtained from Eqs. 6 and 8a, respectively, gives the following result:

$$S' = \frac{S}{u} v_n - \frac{S}{u\rho}(\rho_s v_s + \rho_n v_n) = \frac{S\rho_s}{u\rho}(v_n - v_s). \qquad (13)$$

Similarly, solving Eq. 10a for T' and then substituting expressions for ρ and p' obtained from Eqs. 6 and 9a, respectively, gives the following result:

$$T' = \frac{u}{S\rho}(\rho_s v_s + \rho_n v_n) - \frac{u}{S}v_s = \frac{u\rho_n}{S\rho}(v_n - v_s) \qquad (14)$$

Eliminating $(v_n - v_s)$ from Eqs. 13 and 14 then gives

$$u^2 S' - S^2\frac{\rho_s}{\rho_n}T' = 0 \qquad (15)$$

In Eqs. 12 and 15 pressure and temperature will be used

as the independent variables. The density and entropy will then be eliminated by writing:

$$\rho' = \left(\frac{\partial \rho}{\partial p}\right)_T p' + \left(\frac{\partial \rho}{\partial T}\right)_p T' \qquad (16)$$

$$S' = \left(\frac{\partial S}{\partial p}\right)_T p' + \left(\frac{\partial S}{\partial T}\right)_p T' \qquad (17)$$

The thermal expansion coefficient α is defined as follows:

$$\alpha \equiv \frac{1}{\rho}\left(\frac{\partial \rho}{\partial T}\right)_p \qquad (18)$$

Also the following thermodynamic relations can be shown to hold[12]:

$$\left(\frac{\partial S}{\partial p}\right)_T = -\left(\frac{\partial v}{\partial T}\right)_p = \frac{1}{\rho^2}\left(\frac{\partial \rho}{\partial T}\right)_p = -\frac{\alpha}{\rho} \quad , \qquad (19)$$

and

$$\left(\frac{\partial S}{\partial T}\right)_p = \frac{C_p}{T} \quad . \qquad (20)$$

In Eq. 19, $v = \frac{1}{\rho}$ is the specific volume and in Eq. 20, C_p is the specific heat at constant pressure.

Substituting Eqs. 16 - 20 into Eqs. 12 and 15 then gives:

$$\left[u^2\left(\frac{\partial \rho}{\partial p}\right)_T - 1\right]p' - u^2\rho\alpha T' = 0 \qquad (21)$$

and

$$-\frac{u^2\alpha}{\rho}p' + \left[u^2\frac{C_p}{T} - s^2\frac{\rho_s}{\rho_n}\right]T' = 0 \qquad (22)$$

The coupling, due to the thermal expansion coefficient, between pressure and temperature waves in liquid helium is apparent in Eqs. 20 and 21. If α is neglected in these two equations, pressure and temperature waves will be independent and will propagate with the respective velocities:

$$u_1 = \left(\frac{\partial p}{\partial \rho}\right)^{\frac{1}{2}} \qquad (23)$$

$$u_2 = \left(\frac{TS^2}{C}\frac{\rho_s}{\rho_n}\right)^{\frac{1}{2}} \qquad (24)$$

In Eqs. 23 and 24 no distinction has been made between $(\partial p/\partial \rho)_T$ and $(\partial p/\partial \rho)_S$ or between C_p and C_v because of the following thermodynamic relations[12]:

$$\left(\frac{\partial \rho}{\partial p}\right)_T = \frac{C_p}{C_v}\left(\frac{\partial \rho}{\partial p}\right)_S \qquad (25)$$

$$\frac{C_p}{C_v} = 1 + \frac{\alpha^2 T}{C_p}\left(\frac{\partial p}{\partial \rho}\right)_S \qquad (26)$$

Thus in the approximation that $\alpha = 0$, $(\partial\rho/\partial p)_T = (\partial\rho/\partial p)_S$ and $C_p = C_v$.

B. Coupling Coefficients

The coefficients needed to determine the relative amplitudes of the pressure and temperature waves produced by a given transmitter can now be calculated as follows: In a plane wave the velocities v_s and v_n and the variable parts p' and T' of the pressure and temperature are

proportional to each other. Upon introducing the proportionality factors a, b, and c according to[6]

$$v_n = a v_s \tag{27}$$

$$\rho' = b v_s \tag{28}$$

$$T' = c v_s \tag{29}$$

Equations 10a, 14, 21, and 22 can be written as follows:

$$b - s\rho c = u\rho \tag{30}$$

$$a - 1 = \frac{s\rho}{u\rho_n} c \tag{31}$$

$$\left[u^2\left(\frac{\partial p}{\partial \rho}\right)_T - 1\right] b - \alpha u^2 \rho c = 0 \tag{32}$$

$$\frac{\alpha T u^2}{\rho c_p} b - \left(u^2 - \frac{Ts^2}{c_p}\frac{\rho_s}{\rho_n}\right) c = 0 \tag{33}$$

There will be two sets of the coefficients a, b, and c; one for the case when $u = u_1$ and one for $u = u_2$. When $u = u_1$, Eqs. 30, 31, and 33 can be solved for a_1, b_1, and c_1. The results, to first order in α, are

$$a_1 = 1 + \frac{\alpha\rho}{s\rho_s}\frac{u_1^2 u_2^2}{u_1^2 - u_2^2} \tag{34}$$

$$b_1 = \rho u_1\left(1 + \frac{\alpha T s}{c}\frac{u_1^2}{u_1^2 - u_2^2}\right) \tag{35}$$

$$c_1 = -\frac{\alpha T}{c}\frac{u_1^3}{u_1^2 - u_2^2} \quad . \tag{36}$$

In Eqs. 35 and 36 the subscript has again been left off the specific heat C because no distinction is being made between the specific heat at constant volume and at constant pressure. Doing so would merely introduce terms of higher order in α which have been neglected anyway.

When $u = u_2$, Eqs. 30, 31, and 32 can be solved for a_2, b_2, and c_2. These results, to first order in α, are

$$a_2 = -\frac{\rho_s}{\rho_n} + \frac{\alpha\rho}{s\rho_n}\frac{u_1^2 u_2^2}{u_1^2 - u_2^2} \tag{37}$$

$$b_2 = \frac{\alpha\rho}{s}\frac{u_1^2 u_2^3}{u_1^2 - u_2^3} \tag{38}$$

$$c_2 = -\frac{u_2}{s}\left(1 - \frac{\alpha}{s}\frac{u_1^2 u_2^2}{u_1^2 - u_2^2}\right) \tag{39}$$

In the approximation, $\alpha = 0$, Eq. 34 gives the result, $v_n \cong v_s$. Thus, as expected, in a first sound wave in this approximation the liquid vibrates as a whole in each volume element. For a second sound wave with $\alpha = 0$, Eq. 37 shows that $v_n \cong -\left(\rho_s/\rho_n\right) v_s$. From this it follows that $j = \rho_s v_s + \rho_n v_n = 0$. Thus in a second sound wave in this approximation the superfluid and normal fluid components vibrate out of phase in such a way that the center of mass of each volume element remains stationary.

The coefficients given by Eqs. 34 - 39 can now be used to analyze radiation of pressure and temperature waves from various types of transmitters.

C. Vibrating Solid Surface

The first type of transmitter which will be considered is a plane solid surface lying in the y - z plane and vibrating in the x-direction with velocity given by $u = u_o \exp(i\omega t)$. The superfluid velocity will consist of two components; one associated with waves which propagate at u_1 and the other with waves which propagate at u_2. Solutions in the form of plane waves will be sought. Thus

$$v_s = v_s^{(1)} + v_s^{(2)} \tag{40}$$

$$v_s^{(1)} = A_1 \exp i\omega\left[t - \frac{x}{u_1}\right] \tag{41}$$

$$v_s^{(2)} = A_2 \exp i\omega\left[t - \frac{x}{u_2}\right] . \tag{42}$$

In general, the boundary conditions at a solid surface at rest in liquid helium require that the tangential component of the normal fluid velocity $\vec{v}_n$ and the normal component of the mass flux $\vec{j} = \rho_s \vec{v}_s + \rho_n \vec{v}_n$ vanish. Since only the normal fluid component is associated with the excitations in the liquid the heat flux will be ρSTv_n. The normal component of this heat flux at the surface must equal the heat flow into the surface due to thermal conduction. However, due to the high rate of heat transfer in liquid helium compared with that in a solid, the latter can be neglected. The boundary conditions then reduce

to the vanishing of the normal components of each velocity $\vec{v}_s$ and $\vec{v}_n$. For the vibrating surface the normal components of $\vec{v}_s$ and $\vec{v}_n$ must then equal the velocity of the surface. From Eqs. 27, and 40-42 these boundary conditions give

$$A_1 + A_2 = u_o \tag{43}$$

$$a_1 A_1 + a_2 A_2 = u_o \tag{44}$$

From Eqs. 43 and 44 it then follows that

$$A_1 = \frac{1 - a_2}{a_1 - a_2} u_o \tag{45}$$

$$A_2 = - \frac{1 - a_1}{a_1 - a_2} u_o \tag{46}$$

The amplitudes of the pressure and temperature waves produced in the liquid helium by this vibrating surface are then given, from Eqs. 28, 29, 45 and 46, by

$$p_1' = b_1 A_1 = \frac{b_1(1-a_2)}{a_1-a_2} u_o \tag{47}$$

$$T_1' = c_1 A_1 = \frac{c_1(1-a_2)}{a_1-a_2} u_o \tag{48}$$

$$p_2' = b_2 A_2 = - \frac{b_2(1-a_1)}{a_1-a_2} u_o \tag{49}$$

$$T_2' = c_2 A_2 = - \frac{c_2(1-a_1)}{a_1-a_2} u_o \tag{50}$$

Substituting the expressions for the coefficients from Eqs. 34-39 into Eqs. 47-50 gives

$$p_1' = \left(\rho u_1 - \frac{a\rho u_1 u_2^2}{s}\right) u_o \qquad (51)$$

$$T_1' = \left(\frac{aTu_1}{c}\right) u_o \qquad (52)$$

$$p_2' = \left(\frac{a^2 \rho T u_2^3}{c}\right) u_o \qquad (53)$$

$$T_2' = \left(\frac{aTu_2}{c}\right) u_o \qquad (54)$$

The velocity u_2 is an order of magnitude smaller than u_1 for the temperatures between 1.2 K and T_λ which are of interest here. Thus in obtaining Eqs. 51-54 the approximation $(u_1^2 - u_2^2) \cong u_1^2$ has been used.

D. Fluctuating Temperature Source

The second type of transmitter which will be considered is a surface in the y-z plane whose temperature varies as $T = T_o' \exp(i\omega t)$. The boundary conditions in this case require that the normal component of the mass flux $\vec{j}$ vanish at the surface and that the temperature of the liquid adjacent to the surface equal that of the surface. From Eqs. 27, 29 and 40-42 these boundary conditions give

$$\rho_s(A_1 + A_2) + \rho_n(a_1 A_1 - a_2 A_2) = 0 \qquad (55)$$

$$c_1 A_1 + c_2 A_2 = T_o' \quad . \qquad (56)$$

Solving Eqs. 55 and 56 for A_1 and A_2 yields

$$A_1 = \frac{\rho_s + a_2 \rho_n}{c_1(\rho_s + a_2\rho_n) - c_2(\rho_s + a_1\rho_n)} T_o' \qquad (57)$$

$$A_2 = -\frac{\rho_s + a_1 \rho_n}{c_1(\rho_s + a_2\rho_n) - c_2(\rho_s + a_1\rho_n)} T_o' \qquad (58)$$

The amplitudes of the pressure and temperature waves produced in the liquid helium by this fluctuating temperature plane are then given, from Eqs. 28, 29, 57, and 58 by

$$p_1' = b_1 A_1 = \frac{b_1(\rho_s + a_2\rho_n)}{c_1(\rho_s + a_2\rho_n) - c_2(\rho_s + a_1\rho_n)} T_o' \qquad (59)$$

$$T_1' = c_1 A_1 = \frac{c_1(\rho_s + a_2\rho_n)}{c_1(\rho_s + a_2\rho_n) - c_2(\rho_s + a_1\rho_n)} T_o' \qquad (60)$$

$$p_2' = b_2 A_2 = -\frac{b_2(\rho_s + a_1\rho_n)}{c_1(\rho_s + a_2\rho_n) - c_2(\rho_s + a_1\rho_n)} T_o' \qquad (61)$$

$$T_2' = c_2 A_2 = -\frac{c_2(\rho_s + a_1\rho_n)}{c_1(\rho_s + a_2\rho_n) - c_2(\rho_s + a_1\rho_n)} T_o' \qquad (62)$$

Substituting the expressions for the coefficients from Eqs. 34-39 into Eqs. 59-62 gives

$$p_1' = (a\rho u_1 u_2) T_o' \qquad (63)$$

$$T_1' = \left(\frac{a^2 T u_1 u_2}{c}\right) T_o' \qquad (64)$$

$$p_2' = (-\alpha\rho u_2^2)T_o' \qquad (65)$$

$$T_2' = \left(1 - \frac{\alpha^2 T u_1 u_2}{c}\right) T_o' \qquad (66)$$

E. Vibrating Porous Surface

A third, rather interesting method of generating pressure and temperature waves in liquid helium is that of a vibrating porous surface. The pores are assumed small enough so that, because of its viscosity, the normal fluid cannot flow through them. The condition which must be satisfied in order that this be true is that the normal fluid shear wave penetration depth, $\delta = (2\eta/\rho_n\omega)^{\frac{1}{2}}$, [13] be much larger than the pore diameter. The superfluid, having zero viscosity, can flow through the pores unimpeded.

The plane will again be assumed to lie in the y - z plane and to be vibrating in the x-direction with velocity given by $u = u_o \exp(i\omega t)$. The boundary conditions at this surface require that the normal fluid velocity v_n equal the velocity of the surface and the superfluid velocity v_s be zero. From Eqs. 27 and 40-42 these boundary conditions then give

$$A_1 + A_2 = 0 \qquad (67)$$

$$a_1 A_1 + a_2 A_2 = u_o \qquad (68)$$

Solving Eqs. 67 and 68 for A_1 and A_2 gives

$$A_1 = -A_2 = \frac{u_o}{a_1 - a_2} \qquad (69)$$

To lowest order in α the amplitudes of the pressure and temperature waves produced in the liquid helium by this vibrating porous surface are then given, from Eqs. 28, 29, 69, and 34-39, by

$$p_1' = \frac{c_1}{a_1 - a_2} u_o = (\rho_n u_1) u_o \qquad (70)$$

$$T_1' = \frac{c_1}{a_1 - a_2} u_o = \left(\frac{\alpha T u_1}{c}\,\frac{\rho_n}{\rho}\right) u_o \qquad (71)$$

$$p_2' = -\frac{b_2}{a_1 - a_2} u_o = -\left(\frac{\alpha \rho_n u_2^3}{s}\right) u_o \qquad (72)$$

$$T_2' = -\frac{c_2}{a_1 - a_2} u_o = \left(\frac{u_2}{s}\,\frac{\rho_n}{\rho}\right) u_o \qquad (73)$$

F. Energy Considerations

From Eqs. 51-54 it can be seen that the predominant wave mode produced by the vibrating surface is p_1'. To lowest order the amplitudes T_1' and T_2' are proportional to α while p_2' is proportional to α^2. The amplitude p_1', to lowest order, is not proportional to α. Thus most of the energy radiated by the vibrating surface goes into the p_1' wave. This can also be seen by calculating the intensity of each type of wave. For small oscillations the average kinetic and potential energy densities are

equal. Thus the total energy density in a wave is[14]

$$E = \rho_s v_s^2 + \rho_n v_n^2 = \tfrac{1}{2} A^2(\rho_s + \rho_n a^2). \qquad (74)$$

The intensity is given as usual by the product of energy density and velocity:

$$I = Eu. \qquad (75)$$

From Eqs. 34-39, 45, and 46 the ratio of the intensities I_2 and I_1 of the waves which propagate with the velocities u_2 and u_1, respectively, is

$$\frac{I_2}{I_1} = \frac{u_2 A_2^2(\rho_s + \rho_n a_2^2)}{u_1 A_1^2(\rho_s + \rho_n a_1^2)} \cong \frac{\alpha^2 T u_2^3}{C u_1} \qquad (76)$$

Since α is small, I_2 is much less than I_1. For example, at T = 2.0 K, $I_2/I_1 \cong 2X10^{-6}$.

One tends to regard this result as obvious since a vibrating surface is the basis of any kind of transmitter of ordinary sound. However, as was already mentioned, these results were not known to the early investigators who first attempted to generate second sound with a piezoelectric transducer.[10]

Equations 63-66 indicate that the fluctuating temperature source is a much better transmitter of second sound. Here the amplitude T_2', to lowest order, does not depend on α, while the amplitudes p_1', p_2', and T_1' are proportional to either the first or second power of α. Moreover if

one calculates the ratio of the intensities of the second and first sound waves as before, the result is:

$$\frac{I_2}{I_1} \cong \frac{C}{\alpha^2 T u_1 u_2} \qquad (77)$$

At T = 2.0 K this ratio is $5X10^3$ and increases with decreasing temperature. The first successful observation of second sound resulted when the transmitter was a periodically heated resistor.[10]

III. EXPERIMENTAL

A. Pressure Waves p_1' and p_2' Produced by a Heater

Figure 1 shows the experimental chamber used to investigate the two pressure waves produced in liquid helium by a fluctuating temperature source. It consisted of a cylinder which was closed at one end by a carbon disk resistor and at the other end by a capacitor microphone. Most of the experiments were carried out in a chamber which was 5.7 cm long with a 2.0 cm id. The cylindrical chamber was made by drilling a 2.0 cm hole through a 1.5 inch diameter nylon rod.

The carbon disk resistor, a detailed drawing of which is shown in figure 2, served as the transmitter. It was made by cutting a circular section out of a commercially available carbon resistance strip.[15] This resistance strip consisted of a paper base phenolic laminate with a thin carbon resistance layer permanently bonded to it. The resistance of the carbon layer at room temperature was 1000 ohms per square. A low resistance electrode strip was painted around the periphery of the circular section with silver paint. This electrode was grounded by means of a small screw to the outer conductor of a miniature coaxial cable.[16] The inner conductor of the

A. Outer brass housing
B. Brass ring which holds the Mylar diaphragm down
C. Nylon insulator
D. Brass back plate
E. Aluminized Mylar diaphragm
F. Set screws to adjust the tension in the diaphragm
G. Screws holding the whole chamber to the support rod
H. Stainless steel support rod
I. Copper electrical lead which is connected to the back via a metal spring
J. Carbon disk
K. Nylon cylinder
L. Electrical leads to carbon disk (miniature coaxial cable)

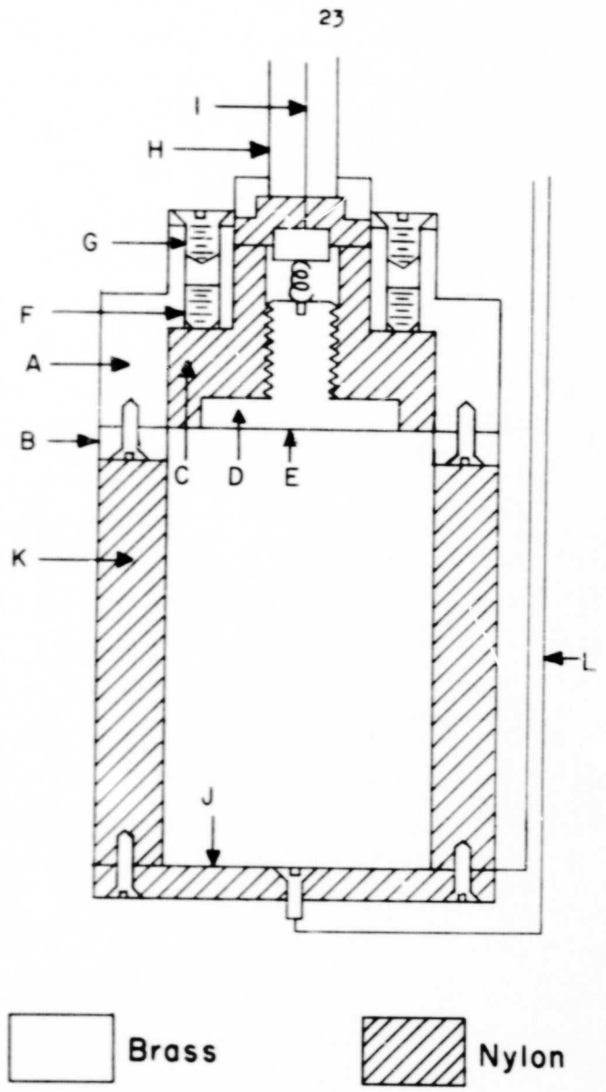

Figure 1 Experimental chamber

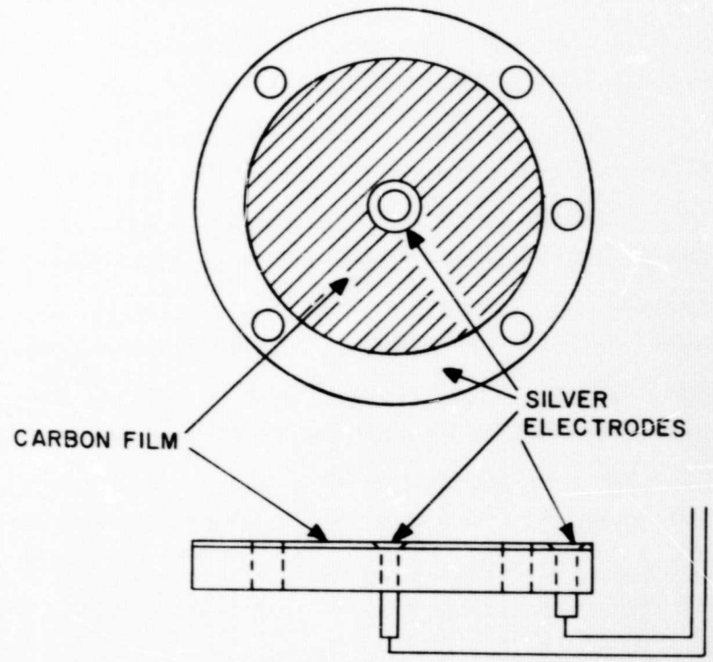

Figure 2 Carbon disk transmitter

coaxial cable was connected to a similar electrode at the center of the disk. The resistance of this carbon disk transmitter at liquid helium temperatures was approximately 600 ohms.

The details of the construction of the capacitor microphone can be seen in Figure 1. A sheet of 0.00025 inch thick Mylar,[17] E, aluminum coated on one side, was stretched over a brass back plate, D. It was held in place with a brass ring, B, which was screwed securely to the brass outer body, A. This also served to ground the aluminum film to the outer body. The back plate was mounted from the outer body by a nylon insulator, C. The back plate and aluminum film formed two plates of a capacitor with the Mylar dielectric in between. Small, 1/32 inch wide, concentric grooves were turned in the surface of the back plate. It was found that doing so would increase the sensitivity of the microphone. The capacitance C_o of the microphone was measured with a capacitance bridge and was found to be 275 picofarads.

The chamber was immersed in a bath of liquid helium and supported by a 0.25 inch od, thin walled, stainless steel tube, H. This stainless steel tube also served as the outer conductor of a coaxial cable. The inner conductor was a no. 32 copper wire, I, which was connected to the back plate of the microphone via a metal spring. The space between the copper wire and stainless steel tube was completely filled with styrofoam spacers. This was

done to reduce noise due to vibrations of the wire. If the wire vibrated, the capacitance of the coaxial cable varied and this would introduce noise in the received signal. The capacitance of this cable was 60 pf.

Small radial grooves were made in the flat surfaces of the brass ring which held the Mylar diaphragm down. This provided passages for the liquid helium to fill the chamber.

The temperature of the liquid helium bath was measured by measuring the vapor pressure and using the 1958 Helium Temperature Scale.[18] The vapor pressure was measured with two Wallace and Tiernan model FA160 absolute pressure gauges. Pressures above 20.0 mm Hg (T = 1.942 K) were measured with a gauge which had a 0 - 50 mm Hg scale. Lower pressures were measured with a gauge which had a 0 - 20 mm Hg scale. Both of these gauges were calibrated against a Hg manometer.

The temperature of the liquid helium was reduced below its boiling point (T = 4.2 K) by pumping with a Heraeus-Engelhard, Model E-225, 147 cfm vacuum pump. The lowest temperature which could be reached in this manner was approximately 1.2 K.

Figure 3 is a schematic diagram of the circuit used with the capacitor microphone. A dc bias voltage of 270 volts was applied, through a series resistor R, between the back plate and aluminum film. When pressure waves impinge upon the diaphragm, the resulting displacement

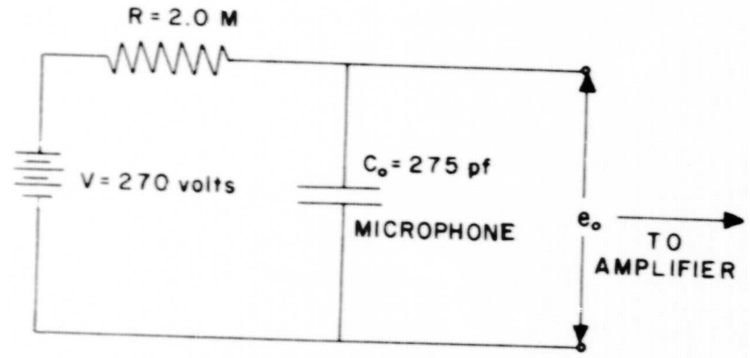

Figure 3 Biasing circuit for the capacitor microphone used as a receiver

of the latter alters the capacitance C_o of the microphone and causes a signal voltage e_o. Resistance R is made large enough so that the capacitor cannot charge and discharge rapidly enough to follow the alternations of capacitance caused by the pressure waves. The condition which must hold for this to be true is that the time constant, RC_o, of the circuit be long compared to the period of the pressure wave.

Assuming the diaphragm to be replaced by an equivalent piston of area A at a distance $x_o + x\sin\omega t$ from the back plate, where x_o is the equilibrium distance, the capacitance will be

$$C = \frac{A}{4\pi(x_o + x\sin\omega t)} \cong \frac{A}{4\pi x_o}\left(1 - \frac{x}{x_o}\sin\omega t\right) = C_o + C'\sin\omega t \ , \quad (78)$$

where $C_o = A/4\pi x_o$ and $C' = -C_o x/x_o$. It has been assumed that $x/x_o \ll 1$.

In the circuit of Figure 3

$$V - iR = \frac{1}{C}\int^t i\,dt \quad (79)$$

Substitution of Eq. 78 into Eq. 79 and differentiation with respect to time gives:

$$(C_o + C'\sin\omega t)R\frac{di}{dt} + (1 + RC'\omega\cos\omega t)i - VC'\omega\cos\omega t = 0 \quad (80)$$

Assuming a solution to Eq. 80 of the form

$$i = A\cos\omega t + B\sin\omega t \quad (81)$$

gives

$$A = \omega RC_o B = \omega VRC' \left[R^2 + \left(\frac{1}{\omega C_o} \right)^2 \right]^{-1} \qquad (82)$$

By using Eq. 82, Eq. 81 can be rewritten as

$$i = \frac{VC'}{C_o} \frac{\sin(\omega t + \phi)}{\left[R^2 + (1/\omega C_o)^2 \right]^{\frac{1}{2}}} \qquad (83)$$

where

$$\tan \phi = \frac{1}{\omega RC_o} \qquad (84)$$

Equation 83 implies that the capacitor microphone may be considered as equivalent to a generator having an open-circuit voltage amplitude VC'/C_o and an internal capacitive impedance $1/i\omega C_o$. The amplitude of the signal voltage e_o will then be

$$e_o = \frac{VC'}{C_o} \frac{R}{\left[R^2 + (1/\omega C_o)^2 \right]^{\frac{1}{2}}} = \frac{VC'}{C_o} \frac{1}{\left[1 + (1/\omega RC_o)^2 \right]^{\frac{1}{2}}} \quad . \qquad (85)$$

Both pulse and standing wave techniques were used to study the pressure waves produced by the heater.

1. Pulse Technique

Figure 4 shows a schematic diagram of the experimental chamber and electronics used in the pulse technique. The input to the carbon disk resistor was a pulse of current consisting of two cycles of a 5.0 kHz signal. This pulse was produced by gating the signal from a General Radio 1310-A oscillator with a General Radio 1396-B tone burst generator.

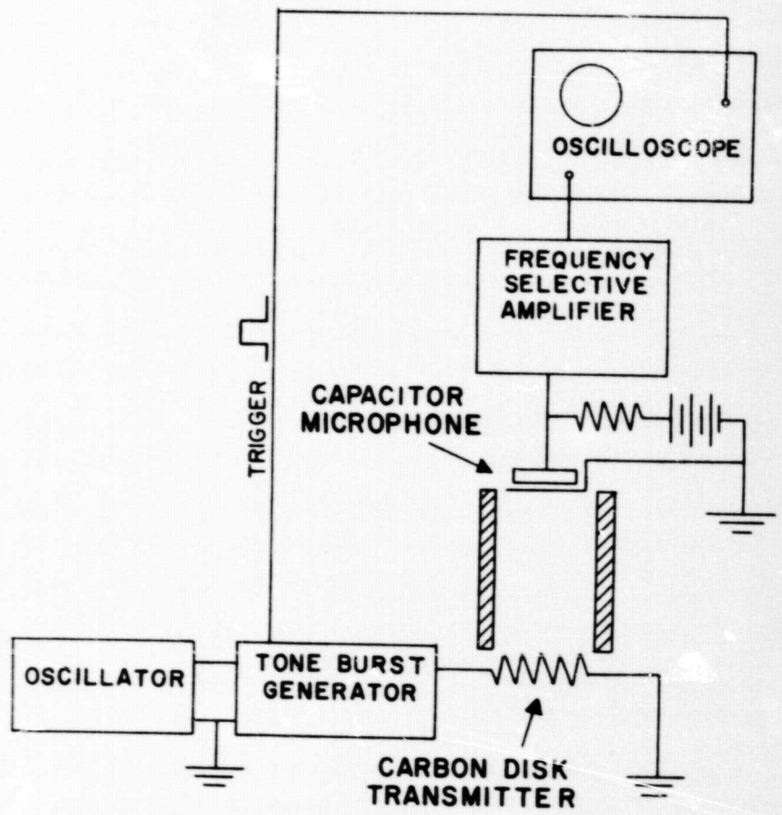

Figure 4 Schematic diagram of the experimental chamber and electronics used in the pulse measurements of p_1' and p_2'.

Since heating occurs on both the positive and negative half cycles of the pulse, the carbon disk transmitter is a frequency doubler. Thus a heat pulse consisting of four cycles of a 10.0 kHz wave was transmitted into the liquid helium. The input power to the heater during a pulse was 25 mW/cm^2. This was the maximum power input which could be used in order to remain in the linear region of received signal versus input power.

The output signal from the microphone was amplified with a Princeton Applied Research, Model 110, variable Q, frequency selective amplifier. Figure 5 shows a plot of relative voltage gain versus normalized frequency for various Q-values of the amplifier. The amplifier was tuned to 10 kHz and the Q-value set at 1. The signal was then fed into a Tektronix Type 531A oscilloscope with a Type 1A1 plug-in amplifier. The oscilloscope trace was triggered simultaneously with the application of the input signal. Figure 6 shows some typical oscilloscope traces obtained in this manner. The times of flight of the pulses labeled p_1' and p_2' verify that they propagated at the velocities of first and second sound, respectively.

The photographs of Figure 6 were taken with a Tektronix C-12 trace recording camera. The tone burst generator was operated in the single burst mode. A fraction of a second before the application of a single driving pulse to the carbon disk transmitter the camera shutter was opened. A single oscilloscope trace was recorded and the

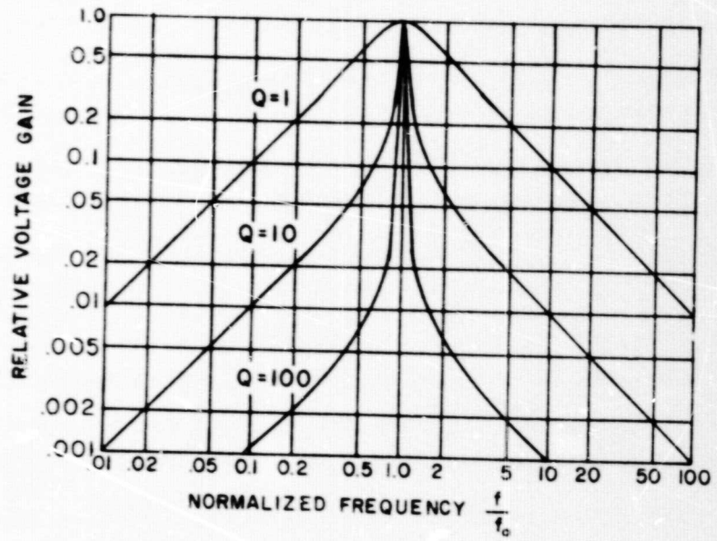

Figure 5 Relative voltage gain of the frequency selective amplifier versus normalized frequency for various Q values.

Figure 6 Some typical oscilloscope traces obtained in the pulse measure-ments of p_1' and p_2'.

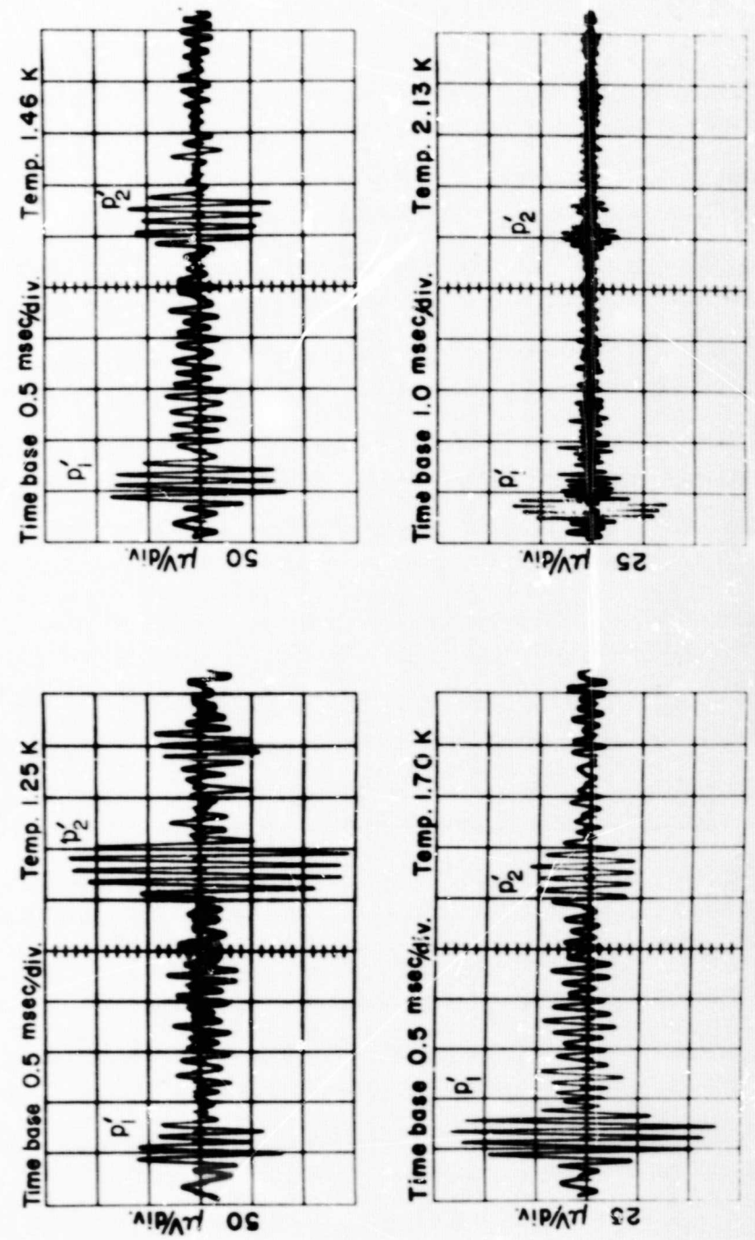

Figure 6

camera shutter closed. All pulse data were taken in this manner.

With the Q of the tuned amplifier set at 1, the received pulses were distorted only slightly and enough filtering was obtained to eliminate most low frequency noise due to vibrations. Subsequent reflections of the p_1' pulse were reduced considerably by drilling many small holes through the carbon disk transmitter and backing. This was necessary because the reflections of p_1' would interfere with the initial p_2' pulse. The smaller pulse appearing after the p_2' pulse in some of the photographs of Figure 6 was due to first sound or p_1' waves being produced at the receiver diaphragm when it was caused to vibrate by the p_2' pulse.

2. Standing Wave Technique

In the standing wave technique the carbon disk transmitter was driven continuously with ac current. In this technique a solid transmitter with no holes drilled in it was used. The frequency was varied until a standing wave resonance of either p_1' or p_2' was observed. All measurements were made with the fundamental resonance, which corresponds to a wavelength equal to twice the length of the cavity. Since u_1 and u_2 are temperature dependent, the fundamental resonance frequency was not constant in these measurements. For waves propagating at u_2 the frequency ranged from approximately 75 Hz to 190 Hz while the range was approximately 1950 Hz to 2050 Hz for waves

propagating at u_1.

It turned out that this method was satisfactory for making quantitative measurements of p_2' but not for p_1'. This is because other resonances, which are believed to be higher harmonics of p_2', were observed at frequencies very close to the fundamental frequency of p_1'. At some temperatures it was difficult to distinguish these resonances from one another. This also made measurement of the Q of the cavity for the p_1' resonances impossible. As will be discussed below the measurement of the Q of the cavity at each resonance is necessary in this technique.

When the frequency of a sound source in a small enclosure equals one of the normal mode frequencies of the enclosure, the amplitude of the pressure variations will be directly proportional to the output of the source and inversely proportional to a damping constant k which is due to losses from absorption and radiation.[19] When the driving frequency does not coincide with, but is close to, the normal frequency the pressure variations build up according to a standard resonance curve. The width of this curve is proportional to k.

In order that the temperature dependence of the output of the source could be studied, the amplitude of the fundamental resonance and the width of the frequency response curve around each resonance were measured as a function of temperature. The width of the resonance

curve was obtained by measuring the amplitude at points off resonance and simultaneously measuring the frequency of the driving oscillator with a Monsanto Model 100A Counter/Timer. A typical resonance curve obtained in this manner is shown in Figure 7. The resonance amplitude in this case was 0.575 mV at a frequency f_o = 127.0 Hz. The ordinate of this graph is relative amplitude; that is, the ratio of the amplitude at frequency f to the amplitude at the resonant frequency f_o. This method of determining the damping constant k was rather tedious. A less time consuming method, which will be described below, was therefore devised.

In this method the driving oscillator was tuned to the resonant frequency but then gated on and off as in the pulse technique. Now, however, many more cycles were included so that the resonance could build up to its maximum amplitude before the driving signal was turned off. Figure 8 shows some typical oscilloscope traces illustrating the response of the cavity to this type of driving current. When the driving current is turned off the amplitude decays with a characteristic exponential envelope e^{-kt}. From this type of photograph the damping constant k and also the amplitude can be measured.

The signals shown in Figure 8 were the result of amplification of the microphone output by the frequency selective amplifier tuned to the resonant frequency and

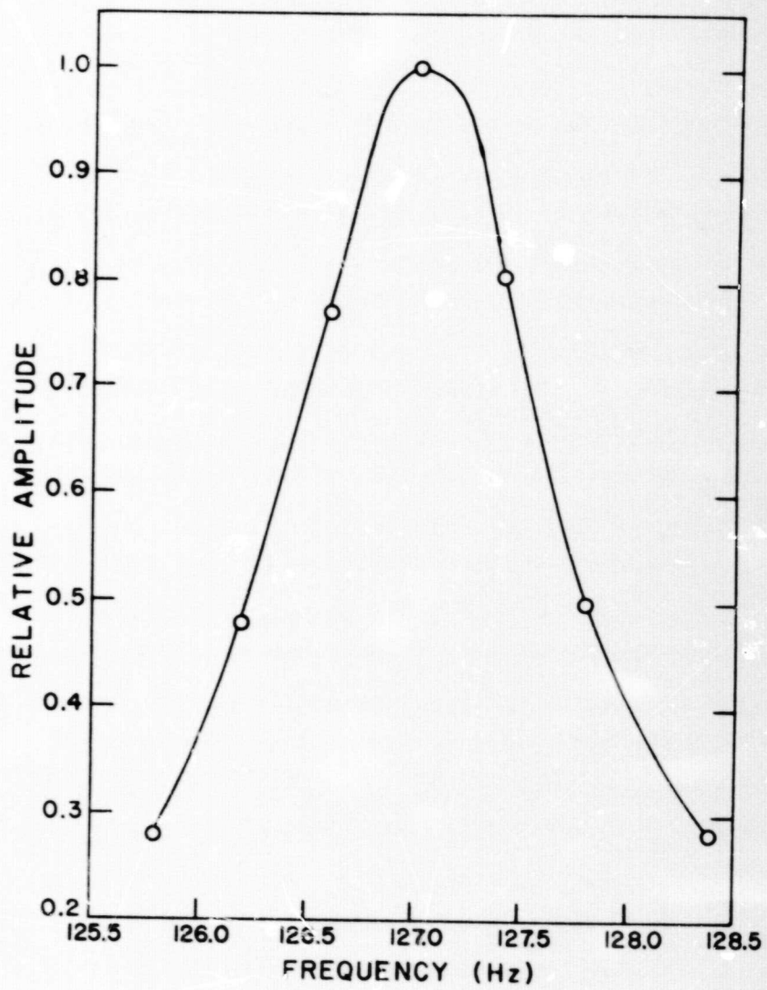

Figure 7 A typical frequency response curve of a standing wave resonance of p_2' at a temperature of 2.06 K.

Figure 8 Some typical oscilloscope traces illustrating the response of the cavity to a long tone burst driving current at the resonant p_2' frequency

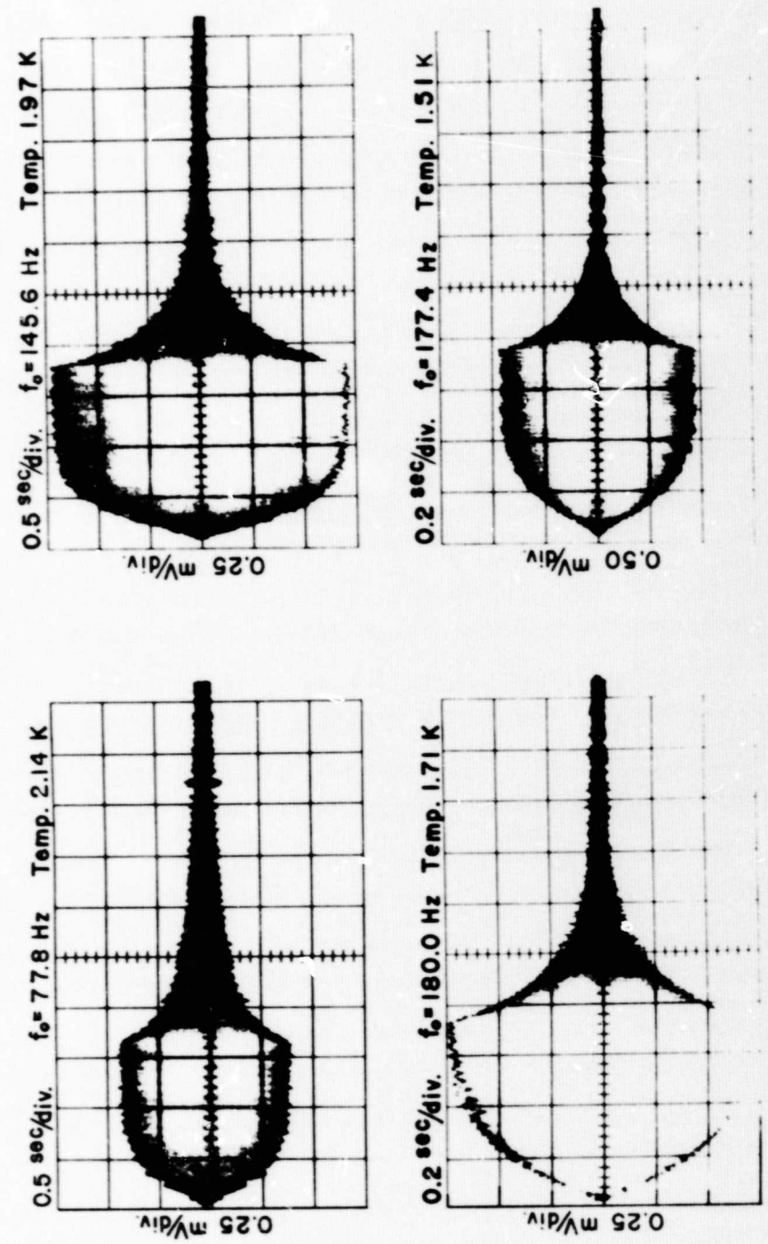

Figure 8

with the Q set at 1. Higher amplifier Q-values could not be used because of the longer time constants associated with the filtering circuitry. However, in the first method in which the width of the resonance curve was measured, the Q of the amplifier could be set at 100.

B. Temperature Wave T_2' Produced by a Microphone

Initially an attempt was made to observe the temperature waves produced by a microphone by merely interchanging the transmitter and receiver in the apparatus already described (Figure 1). The capacitor microphone was driven with ac voltage and the carbon disk resistor was used as a second sound receiver. When used for this purpose a constant current I = 1.0 ma was maintained in the carbon disk. This was accomplished by connecting it in series with another resistor, R, much greater than the disk resistance, and a dry cell. The temperature variations in the second sound wave cause the resistance of the disk to vary and this results in a signal voltage.

Extremely weak signals, barely visible above the noise, were observed with this arrangement by using standing waves. The signals were too weak for quantitative measurements to be made. However, these waves were able to be studied quantitatively by using a new type of second sound transducer as receiver.

1. Porous Diaphragm Second Sound Transducer

This transducer was identical to the capacitor microphone already described except that the aluminized Mylar

diaphragm was replaced by a diaphragm made from a porous filter material.[20] A conducting layer of aluminum was vacuum deposited on one side of the filter.

This aluminum film was deposited on the filter with a standard vacuum deposition apparatus consisting of a high vacuum bell jar chamber at the base of which was mounted a tungsten filament. The filaments were Edwards High Vacuum Inc., Type A10 tungsten filaments. The filter was mounted by means of a cardboard ring and masking tape on a glass microscope slide. The slide was then mounted approximately four inches above the tungsten filament with the filter facing the filament. Another microscope slide was mounted next to the one which was holding the filter. The purpose of this second slide was to provide a means of observing how much aluminum was being deposited. A few strips of high purity aluminum wire were hung from the tungsten filament.

The procedure used to deposit the aluminum film on the filter was as follows: 1). The bell jar was pumped down to a vacuum of 10^{-4} micron. 2). The current to the filament was switched on and increased to approximately 30 amps. At this current the aluminum strips would melt and wet the whole filament in about 15 - 30 seconds. 3). The current was then increased to approximately 40 amps, while observing the plain microscope slide through the bell jar. At a current of 40 amps this plain slide would be coated with a totally reflecting layer of

aluminum in 5 - 10 seconds. 4). As soon as it was observed that this layer was totally reflecting the current was switched off. This provided a satisfactory conducting layer of aluminum on the filter.

When the leads of an ohmmeter were applied at opposite points of the periphery of a 47 mm diameter filter coated in this way the measured resistance was 10 - 20 ohms. Sherlock and Edwards[21] have conducted tests of the flow rate and bubble point pressure of the same type of filters on which a conducting layer of gold had been vacuum deposited. They found no significant reduction in either the number of open pores or the pore diameter. It is assumed that this is also the case with the filters used in this investigation.

The pore size of the filter material was specified by the manufacturer to be 0.45 ± 0.02 micron. The capillary pores occupy approximately 80% of the total filter volume. If the normal fluid shear wave penetration depth, $\delta = (2\eta/\rho_n\omega)^{\frac{1}{2}}$,[13] is much larger than the pore size, then flow of the normal fluid through the pores is impeded. However, the superfluid component, having zero viscosity, can flow through the pores unimpeded.

As was shown previously, in the first approximation, second sound consists of the normal fluid and superfluid components oscillating out of phase in such a way that the net density or pressure fluctuation is zero. Thus a second sound wave impinging on the porous diaphragm will

exert a force on it.

It should be pointed out that this transducer will also be sensitive to pressure waves. This must be taken into account when interpreting signals received with it.

This type of transducer has been used to study the velocity of second sound close to the λ-point[22] and also to study second sound in ^3He - ^4He mixtures below 0.3 K.[23] In these experiments the principle advantage of this type of transducer was that it was an efficient transmitter and receiver of second sound without introducing heating. A detailed study of these transducers has been made by Sherlock and Edwards.[21]

An experiment was devised to test the sensitivity of this transducer. The details of this experiment will be described in detail in Section IV-E below. The results were that, in addition to the above mentioned desirable properties, this transducer was also much more sensitive to second sound temperature fluctuations than the carbon resistance receiver described above.

2. Apparatus and Procedure for Measuring T_2'

The investigation of the temperature waves produced by a vibrating diaphragm was carried out with the experimental chamber previously described (Figure 1) except that the regular capacitor microphone replaced the carbon disk as transmitter and the porous diaphragm transducer was the receiver. The biasing circuit shown in Figure 3 was also used with the porous diaphragm receiver in this experiment.

Even with the increased sensitivity of the porous diaphragm receiver the second sound waves produced by the microphone could only be observed with the standing wave technique. Again the amplitude of the fundamental resonance and the damping constant were measured as a function of temperature. The damping constant was determined by measuring the width of the frequency response curve around each resonance. The alternate method of observing the decay of a long tone burst could not be used because the Q of the tuned amplifier had to be set at 50 or higher in order to make accurate measurements of the signal amplitude.

The regular capacitor microphone transmitter was driven with 30 volt peak ac voltage. In addition a 170 volt dc bias voltage was applied in order to increase the output. The fact that this dc bias will increase the output can be seen as follows. Under the action of an applied force $F = F_o \sin(\omega t)$ the diaphragm of the microphone will execute harmonic vibrations of frequency ω with its velocity amplitude u_o given by[24]:

$$u_o = \frac{F_o}{Z_m + Z_r} \qquad (86)$$

where Z_m is the mechanical impedance of the diaphragm and Z_r is the acoustic radiation impedance of the liquid helium. The dc bias voltage was again applied through a large series resistor, as indicated in Figure 9, so that

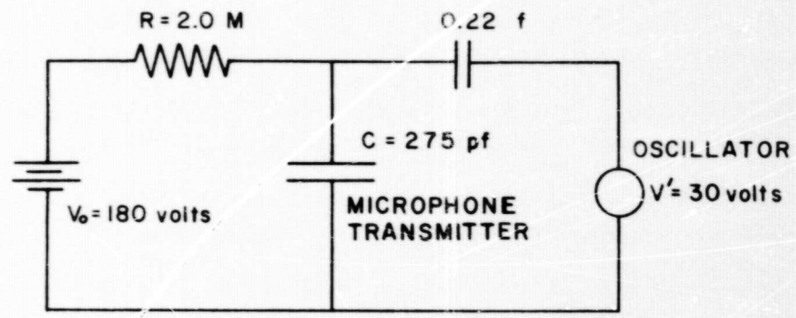

Figure 9 Biasing circuit for the capacitor microphone used as a transmitter.

charge could be assumed to be constant. The purpose of the 0.22 μf capacitor in the circuit in Figure 9 is to block the dc voltage from the oscillator. The impedance of this capacitor is negligibly small compared to that of the microphone. The force between the aluminized side of the diaphragm and the back plate will be

$$F = \frac{2\pi Q^2}{A} = \frac{2\pi C_o^2}{A} V^2 \qquad (87)$$

where Q is the charge, C_o the capacitance, A the area of the diaphragm, and V the potential difference between the aluminized side of the diaphragm and the back plate. In this case $V = V_o + V'\sin\omega t$ so that

$$F = \frac{2\pi C_o^2}{A}\left[V_o^2 + 2V_oV'\sin(\omega t) + (V')^2\sin^2(\omega t)\right]$$

$$F = \frac{2\pi C_o^2}{A}\left[V_o^2 + \frac{(V')^2}{2} + 2V_oV'\sin(\omega t) - \frac{(V')^2}{2}\cos(2\omega t)\right]. \quad (88)$$

If $V_o = 0$ then $F = \pi C_o^2(V')^2/A - (\pi C_o^2(V')^2/A)\cos(2\omega t)$. The term $\pi C_o^2(V')^2/A$ is just a constant and therefore the microphone will produce pressure and temperature waves whose frequency is double that of the driving voltage. This is physically clear because both the positive and negative half cycles of the driving voltage produce attraction between the diaphragm and back plate. However, if V_o is several times larger than V' the coefficient of $\sin(\omega t)$ in Eq. 88 will be much larger than that of $\cos(2\omega t)$. The microphone will then produce waves whose

frequency is equal to that of the driving voltage and whose amplitude is much larger than those produced when $V_o = 0$.

IV. RESULTS

A. Pressure Waves p_1' and p_2' Produced by a Heater

1. Output Amplitude Data From Microphone

In the pulse technique the amplitudes of the pressure pulses p_1' and p_2' (Figure 6) were measured as a function of temperature. The corrections to these data due to the attenuation of first and second sound were negligibly small. A plot of the data is shown in Figure 10. On Figure 10 the squares represent p_1' pulse amplitude measurements and the circles p_2' pulse amplitude measurements. Also included on this plot are data from the standing wave measurements of p_2'. These are represented by the triangles. The ordinate of this graph is the amplitude of the ac output voltage of the microphone from the pulse experiments. As will be discussed below, the standing wave data have been reduced by a constant factor in order that they could be displayed on the same graph as the pulse data on Figure 10.

Figure 11 shows a separate plot of the actual p_2' standing wave resonance amplitude as a function of temperature. These amplitudes are, of course, larger than the amplitudes of the p_2' pulses. The damping constant of each resonance was measured both by measuring the width

Figure 10 The pressure wave amplitudes p_1' and p_2' produced by the carbon disk transmitter, plotted versus temperature.

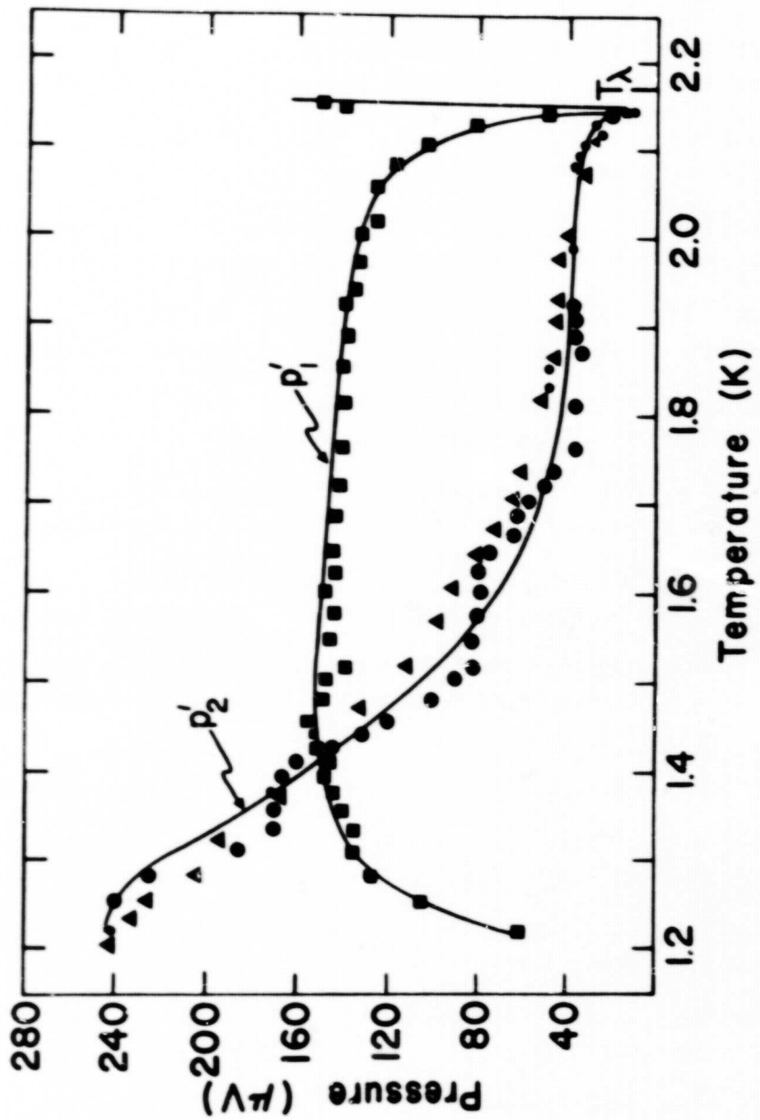

Figure 10

Figure 11 The p_2' standing wave resonance amplitude plotted versus temperature.

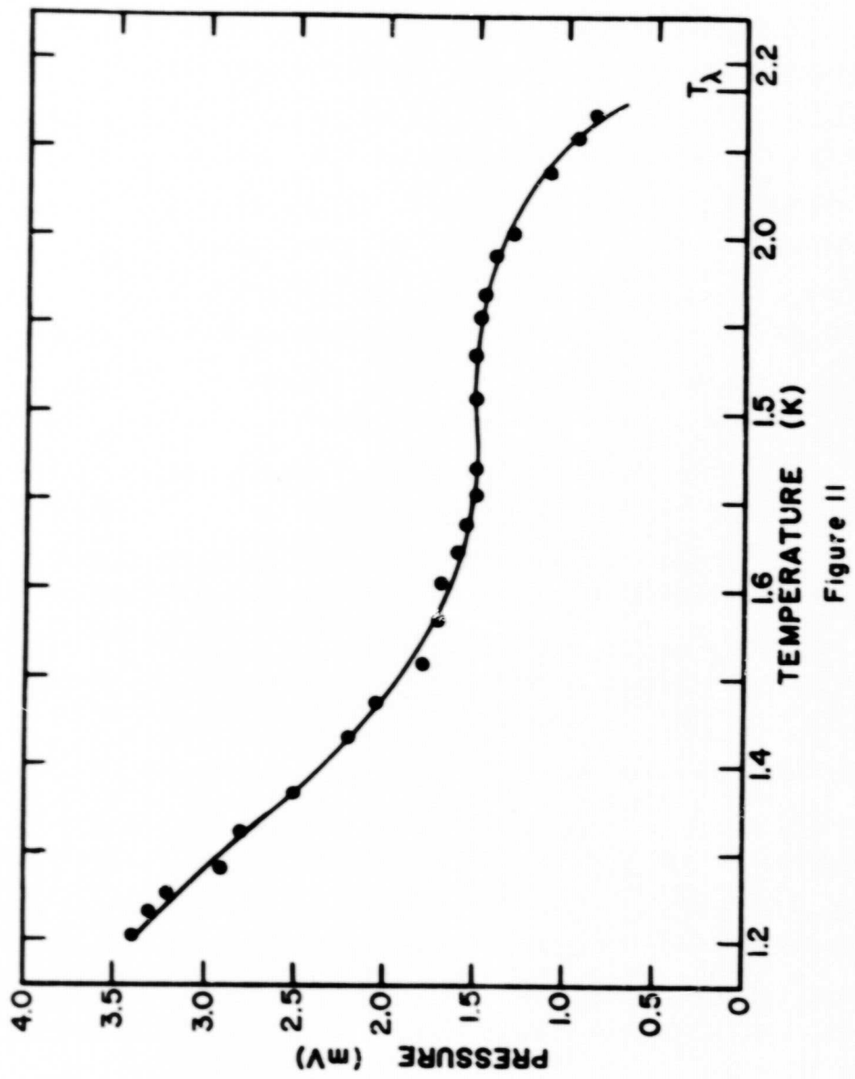

Figure 11

of the frequency response curve around each resonance and by the decay of a long tone burst driving signal at the resonant frequency. Figure 12 shows a plot of the damping constant k measured by both of these methods.

The circles represent the experimental values of k obtained by measuring the width of the frequency response curve, (see Figure 7). In this case $k = \pi(f'' - f')$ where f' and f" are the frequencies at which the amplitude is $1/\sqrt{2}$ times its value at resonance. The squares represent the values of k obtained from the decay of a long tone burst driving signal as illustrated in Figure 8. The time it takes for the amplitude to decay to 1/e of its maximum is equal to 1/k.

The resonance amplitude is directly proportional to the source output and inversely proportional to the damping constant.[24] Thus the amplitude data of Figure 11 must be corrected with the data of Figure 12 in order to obtain the temperature dependence of the source output from the standing wave measurements. The data represented by triangles in Figure 10 are the result of correcting the amplitude data of Figure 11 for the variation of the damping constant data in Figure 12 and then dividing by a constant factor.

The values for the attenuation of second sound derived from the damping constant data of the standing wave measurements, (see Figure 12), are larger than the published values.[25-27] This is not surprising, however, because

Figure 12 The damping constant of p_2' standing waves plotted versus temperature.

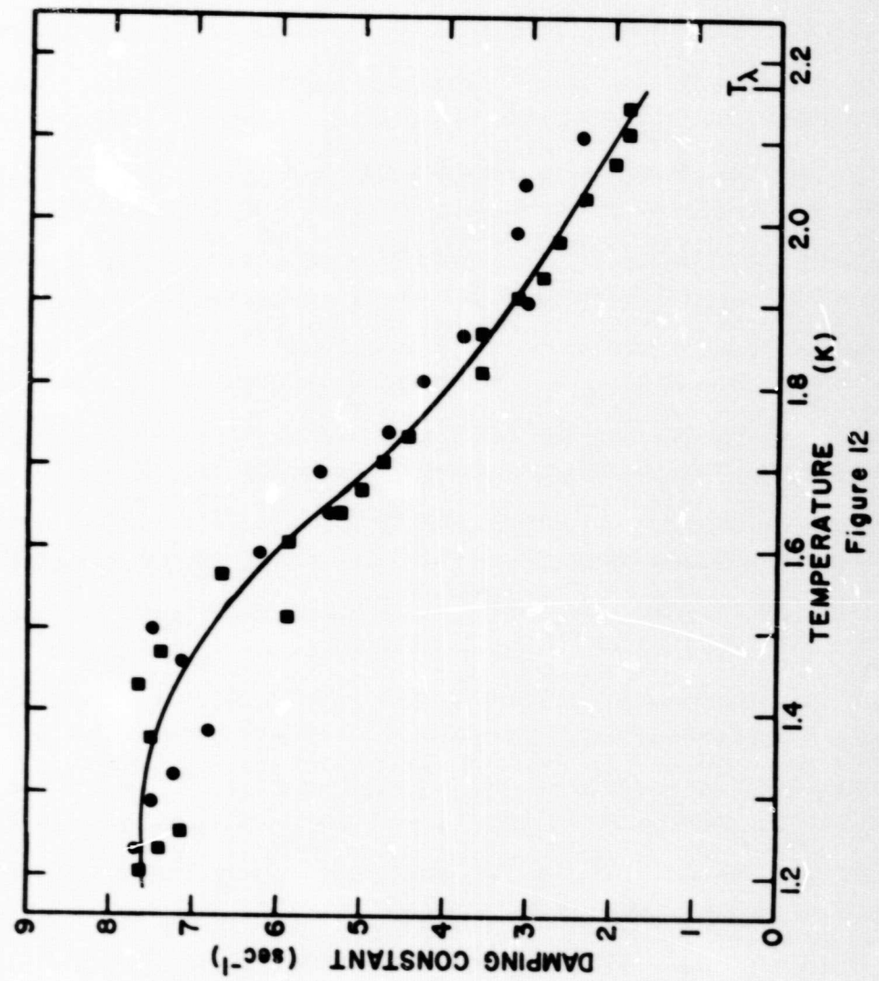

Figure 12

In the standing wave experiments there are losses due to reflection and radiation in addition to absorption in the liquid. Experiments whose purpose it is to measure the attenuation of second sound are specifically designed to minimize the first two types of losses.

In Figures 10 - 12 the solid lines are merely smooth curves drawn through the data points. In Figures 10 and 11 the units on the ordinate are microvolts and millivolts, respectively, because the capacitor microphone was not calibrated. The output voltage will be proportional to the pressure wave amplitude.

3. Temperature Amplitude T_o Produced by the Carbon Disk Transmitter

Before the experimental p_1' and p_2' data of Figure 10 can be compared with the theoretical expressions of Equations 63 and 64 the following must be considered: As previously indicated in Section II, the heat transport is associated with the normal component and is given by[1,2]:

$$\dot{Q} = \rho S T v_n \quad . \tag{89}$$

The units of $\dot{Q}$ are energy per square centimeter per second. An approximate relation between $\dot{Q}$ and the amplitude of the temperature variation in a second sound wave will now be derived.

Solving Eq. 14 for $(v_n - v_s)$ and letting $u = u_2$ gives

$$v_n - v_s = \frac{s\rho}{u_2 \rho_n} T_2' \quad . \tag{90}$$

In the approximation that $\alpha = 0$ it was shown, in Section II, that for a second sound wave

$$u_2^2 = \frac{TS^2}{C} \frac{\rho_s}{\rho_n} \quad , \tag{91}$$

and

$$J = \rho_s v_s + \rho_n v_n = 0 \quad . \tag{92}$$

Solving Eq. 92 for v_s and substituting this into Eq. 90 gives

$$v_n \left(1 + \frac{\rho_n}{\rho_s}\right) = \frac{s\rho}{u_2 \rho_n} T_2' \quad . \tag{93}$$

Solving Eq. 93 for v_n and using $\rho = \rho_s + \rho_n$ and Eq. 91 gives

$$v_n = \frac{s\rho_s}{u_2 \rho_n} T' = \frac{Cu_2}{TS} T_2' \quad . \tag{94}$$

Substituting Eq. 94 into Eq. 89 then gives

$$\dot{Q} = \rho C u_2 T_2' \quad , \tag{95}$$

or

$$T_2' = \frac{\dot{Q}}{\rho C u_2} \quad . \tag{96}$$

In the measurements of p_1' and p_2' the input power to the carbon disk transmitter was constant. Therefore $\dot{Q}$ was constant. In the earlier analysis of the pressure waves produced by a fluctuating temperature source the

transmitter was considered to be a plane surface whose temperature varied as $T = T_0 \exp(i\omega t)$. However, because the power input to the carbon disk transmitter was constant, and because of Eq. 96, T_0 is itself a function of temperature in this experiment. It is given, from Eqs. 66 and 67, by $T_0 = \frac{1}{2}\rho c u_2$.

The theoretical expression of Eq. 96 was verified by using the following experiment. In the experimental chamber of Figure 1 the capacitor microphone was replaced by a second carbon disk resistor identical to the transmitter. This resistor served as a receiver of the second sound wave T_2' produced by the carbon disk transmitter. A schematic diagram of the experimental apparatus in this case is shown in Figure 13. A constant current I = 1.0 ma was maintained through the receiver R by means of a dry cell in series with a resistor R_1 which was much larger than R. The temperature fluctuation T_2' causes the resistance of the receiver to vary and this produces the output voltage

$$e_0 = I \frac{dR}{dT} T_2' \qquad (97)$$

The resistance of the receiver as a function of temperature, dR/dT, was obtained by measuring the dc voltage across R due to the 1.0 ma dc current. This voltage was measured with a Leeds and Northrup type K-3 potentiometer. The result was that the average value of dR/dT from 1.2 K

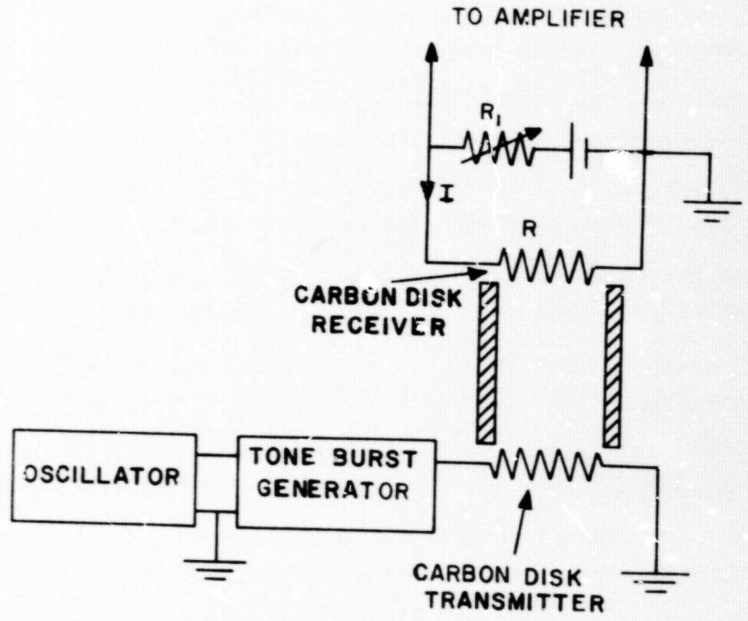

Figure 13 A schematic diagram of the apparatus used to measure the second sound amplitude T_2' produced by the carbon disk transmitter.

to T_λ was approximately 70 Ω/K.

Both the previously described pulse and standing wave methods were used to investigate the temperature dependence of T_2'. The input power to the carbon disk transmitter was again 25 mW/cm^2 which is the same as was used in the measurement of the pressure amplitudes p_1' and p_2' produced by this transmitter.

The results of these measurements are shown in Figure 14. The solid line is the theoretical curve of $\xi/\rho c u_2$ with ξ = 25 mW/cm^2. The published measured values of density,[28] specific heat,[29,30] and velocity of second sound[31-33] were used. The data represented by circles in Figure 14 are measurements of T_2' obtained by the pulse method and the squares represent standing wave measurements. Again, as in the standing wave measurements of p_2', the amplitude of the fundamental T_2' standing wave resonance, and the damping constant k were measured as a function of temperature. The standing wave data on Figure 14 have been corrected for variation of the damping constant k and have been reduced by a constant factor so that they could be plotted on the same scale with the pulse data.

The experimental values of T_2' from the pulse measurements on Figure 14 were obtained from Eq. 97 and the measured values of e_o and I(dR/dT). The scale on the right hand side of Figure 14 is labeled with the corresponding values of e_o in microvolts. Good agreement is indicated between both the pulse and standing wave T_2' data and the theoretical curve.

Figure 14 The second sound amplitude T_2' produced by the carbon disk transmitter, plotted versus temperature.

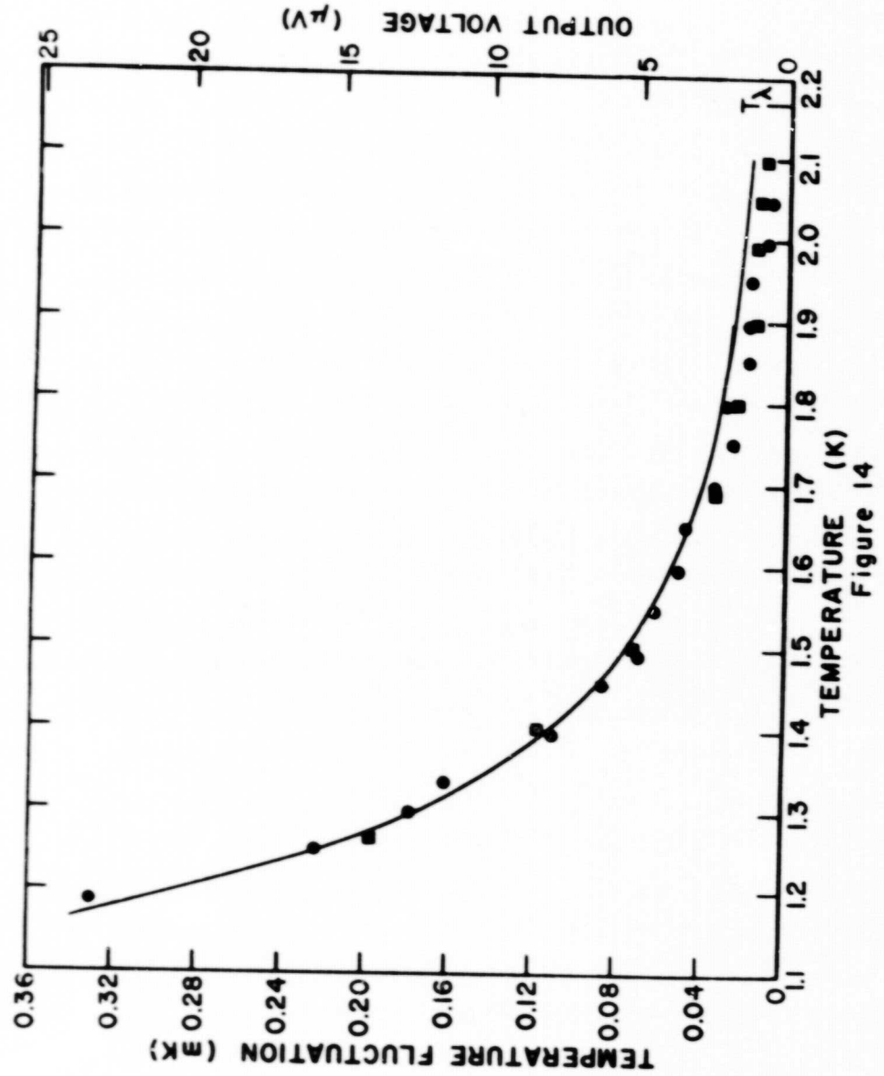

Figure 14

3. Output Amplitude Data Corrected For Variation of T_o.

Figure 15 shows the results of dividing the p_1' data in Figure 10 by the T_2' data in Figure 14. Since the temperatures of the data points in the two experiments did not coincide, the points used for Figure 15 were taken from smooth curves drawn through the data. In Figure 15 the solid line is the theoretical curve of $p_1'/T_o = \alpha\rho u_1 u_2$ from Eq. 63. Since the capacitor microphone was not calibrated, the experimental data have been normalized to agree with the theoretical curve at T = 1.4 K. In this way the temperature dependence of the data could be compared with the theory. Reasonably good agreement between the experimental data and the theoretical curve is indicated.

Figure 10 shows a sudden sharp increase in p_1' just below the λ-point. The temperature measurements in these experiments were not sophisticated enough to determine with great accuracy at what temperature this sharp increase in p_1' occurred. However it was definitely below the λ-point. This phenomenon is not predicted by the theory based on the linearized two-fluid hydrodynamic equations. No satisfactory explanation for this phenomenon has been found. It is believed to be associated with nonlinearities near the λ-point.

The p_1' amplitude continues to increase through the λ-point and then levels off at a value which is much higher than that below T_λ. Thus a fluctuating heat source

Figure 15 A plot of the p_1' data on Figure 10 divided by the T_2' data on Figure 14.

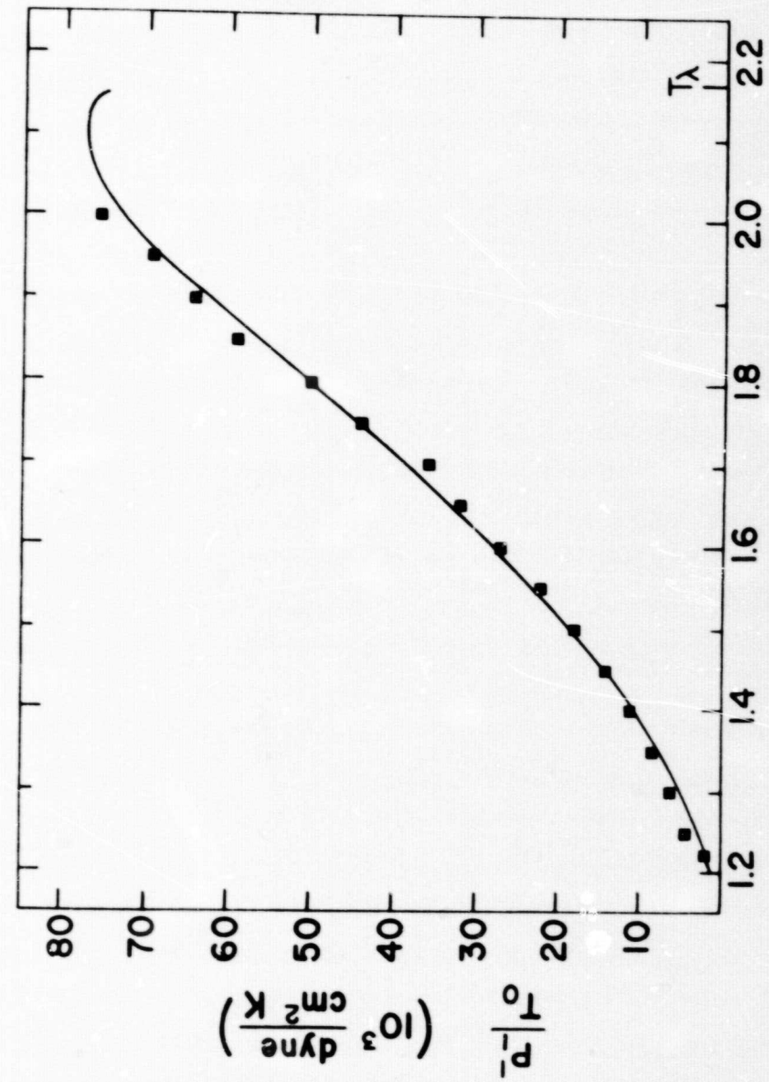

Figure 15

is useful as a transmitter of ordinary sound in liquid helium both above and below the λ-point. The generation of sound waves by a fluctuating heat source has long been known in gases[34-37] and liquids[38] and is known as the thermophone effect.

Figure 16 shows the results of dividing the p_2' data in Figure 10 by the T_2' data in Figure 14. Again the data points in Figure 16 were obtained from smooth curves drawn through the data in Figures 10 and 14 because the temperatures of the data points from these two experiments did not coincide. In Figure 16 the solid line is the theoretical curve of $p_2'/T_o = -\alpha\rho u_2^2$ from Eq. 65. The dashed line represents a correction to Eq. 65 due to the viscosity of the normal fluid and the coefficient of second viscosity ζ_2. This correction will be discussed in greater detail in Section V-A below. Here the data have been normalized to agree with the theoretical curve at the maximum in order that the temperature dependence of the two could be compared. From Figure 16 disagreement between the experimental data and the theory is apparent.

This discrepancy between the temperature dependence of the experimental p_2' data and the theoretical curve was not unexpected for the following reason. An inspection of Eqs. 63 and 65 shows that the ratio of p_2' to p_1' should be

Figure 16 A plot of the p_2' data on Figure 10 divided by the T_2' data on Figure 14.

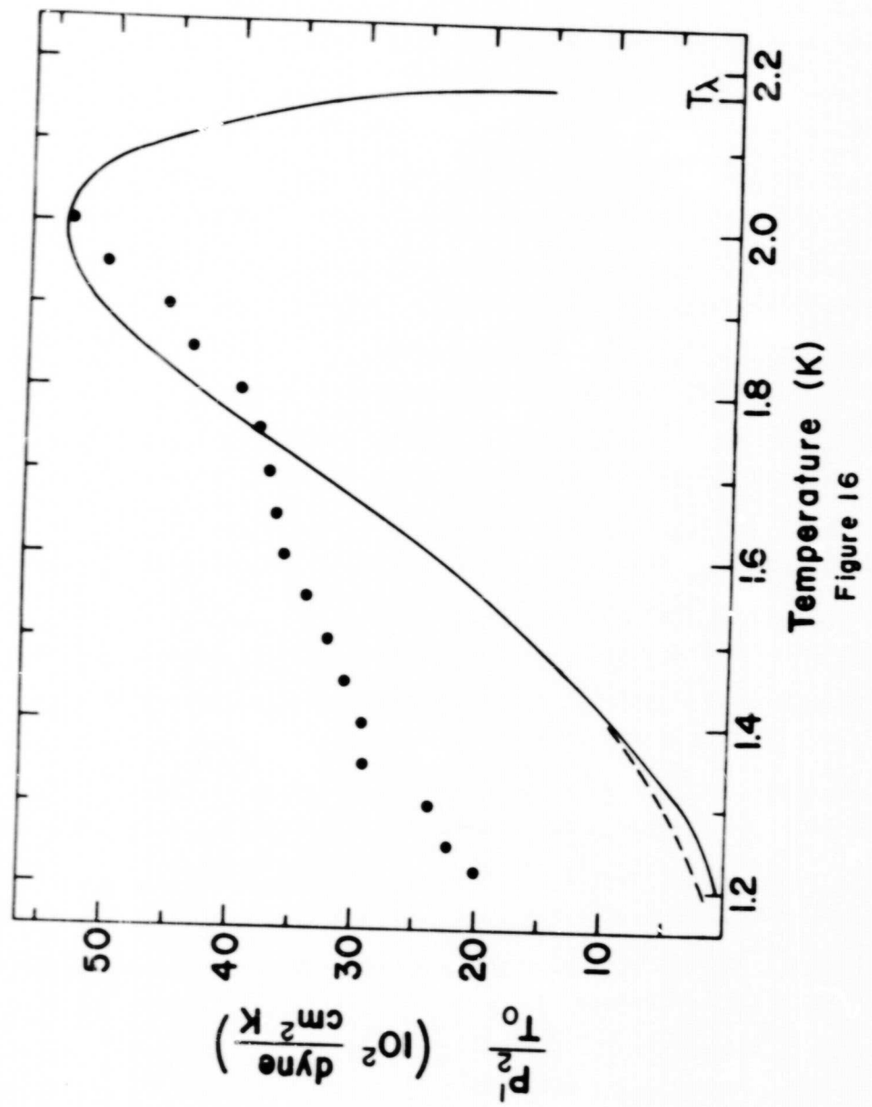

Temperature (K)
Figure 16

$$\frac{p_2'}{p_1'} = \frac{u_2}{u_1} \quad . \tag{98}$$

In the temperature range of these investigations $u_2 < 0.1\ u_1$ so that p_2' should be less than $0.1\ p_1'$. However, as can be seen in Figure 10, the results of this investigation show that p_2' is the same order of magnitude as p_1'.

In addition, the thermal expansion coefficient of liquid helium changes sign at T = 1.17 K.[28] Therefore, according to Eqs. 67 and 65, the amplitudes p_1' and p_2' should be zero at this temperature. Although this temperature could not quite be reached in the cryostat used in these experiments, the results on Figures 10, 15 and 16 indicate that p_2' is not zero at this temperature but that p_1' is.

Thus it appears that the experimental p_1' data follow the theoretical predictions but that there is a contribution to p_2' which has not been accounted for.

B. Temperature Wave T_2' Produced by a Microphone

1. Sensitivity of the Porous Diaphragm Transducer

As previously indicated, the temperature wave T_2' produced by the vibrating diaphragm of a regular capacitor microphone was observed by using, as a receiver, a transducer similar to a capacitor microphone. The active element of this transducer was a porous diaphragm made from metallized filter material. The sensitivity of this transducer to temperature waves was investigated by using it as

a receiver of the second sound waves produced by a carbon disk transmitter.

The experimental chamber used in this experiment was identical to the one used in the investigations of the pressure waves p_1' and p_2' and described in Figure 1, except that the diaphragm of the receiver was made from the porous filter material. The same carbon disk transmitter and electronics as described in Figure 3 and 4, respectively, were used. The power input to the transmitter was again 25 mW/cm^2. The amplitude of the second sound waves produced by the carbon disk heater was again measured in this experiment by both the pulse and standing wave methods.

The results of these measurements are shown in Figure 17. The solid line is again the theoretical curve of $\dot{q}/\rho c u_2$ with $\dot{q}$ = 25 mW/cm^2. The data represented by circles in Figure 17 are measurements obtained by the pulse method and the squares represent standing wave measurements. As in Figure 14, the ordinate on the left hand side of Figure 17 is labeled with temperature fluctuations in millikelvins. The ordinate on the right is labeled with peak output voltage in millivolts from the porous diaphragm transducer. The standing wave data in Figure 17 have again been corrected for variation of the damping constant and reduced by a constant factor so they could be plotted on the same graph with the pulse data.

Comparison of the ordinates on the right hand sides of Figures 14 and 17 shows that the porous diaphragm

Figure 17 The output voltage from the porous diaphragm transducer used as a receiver of the second sound waves produced by the carbon disk transmitter, plotted versus temperature.

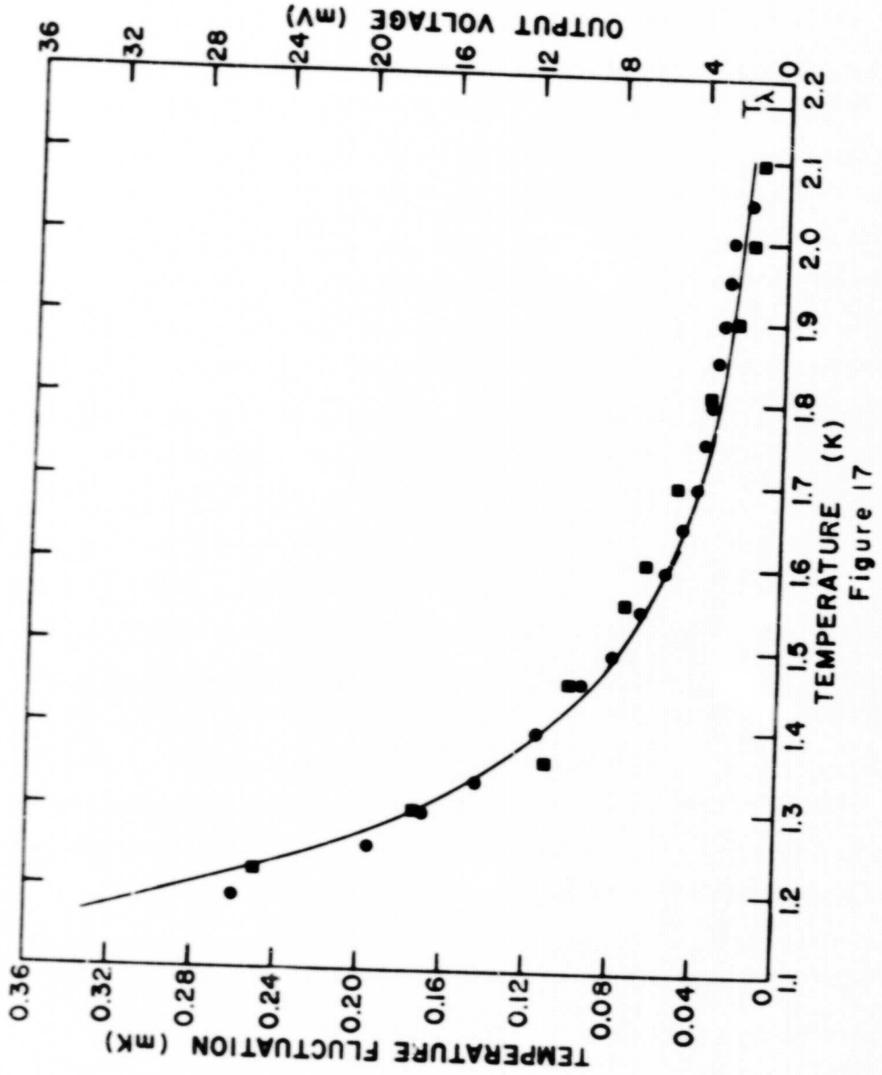

Figure 17

transducer was approximately 1000 times more sensitive to second sound temperature fluctuations than the carbon disk resistor. The data from these two experiments do, in fact, constitute a calibration of the porous diaphragm transducer. Thus the sensitivity in Volts/Kelvin of this transducer can be obtained from the data in Figures 14 and 17. Only a slight variation with temperature of this sensitivity is indicated from these data.

2. Measurement of T_2'

Figure 18 shows the results of the standing wave measurements of the second sound amplitude T_2' produced by the regular capacitor microphone and received by the porous diaphragm transducer. The solid line is the theoretical curve of $T_2'/u_o = \alpha T u_2/C$ from Eq. 54. The magnitude of u_o was not known so the experimental data have been normalized to agree with the theoretical curve at $T = 1.4$ K. In this way the temperature dependence of the experimental data could be compared with that of the theoretical curve.

The dashed line in Figure 18 is the theoretical curve of T_2'/u_o which results when the contribution from the viscous forces at the chamber walls is taken into account. These forces are due to the viscosity η of the normal fluid component. This correction will be discussed in more detail in Section V-B below. There is fair agreement between the experimental data and the theoretical curve at lower temperatures but a large discrepancy at higher

Figure 18 The second sound amplitude T_2' produced by the capacitor microphone, plotted versus temperature.

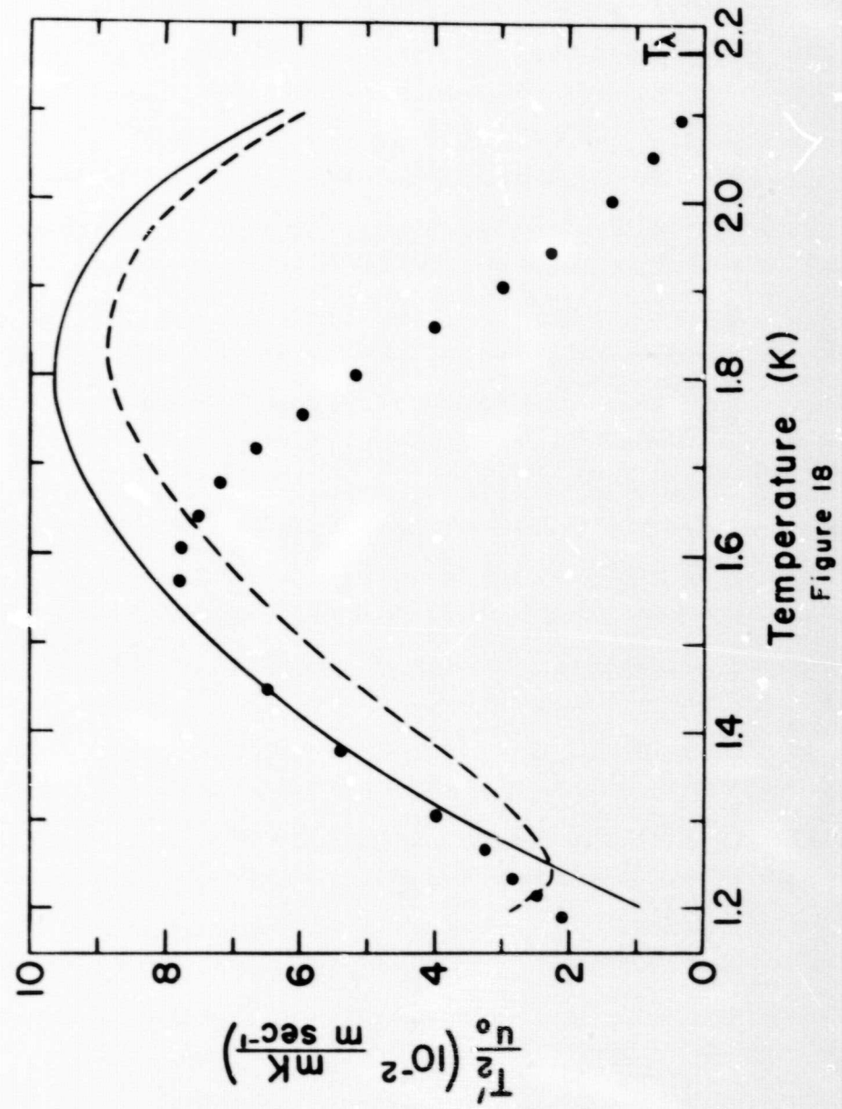

Figure 18

temperatures.

In this experiment plane wave resonances corresponding to waves which propagate at the velocity of first sound u_1 were also observed. The amplitudes of these resonances were an order of magnitude larger than the T_2' resonances. Since the porous diaphragm receiver will also respond to pressure waves, it is not clear whether these are resonances of p_1' of Eq. 51, or of T_1' of Eq. 52, or both. To answer this question the relative sensitivity of the porous diaphragm transducer to pressure and temperature waves would have to be known. This same question must, in fact, be considered in connection with the T_2' resonances. There may be a contribution to these resonances from p_2' of Eq. 53.

This question of the relative sensitivity of the porous diaphragm transducer to pressure and temperature waves, and the contribution of the various wave modes to the resonances observed in this experiment will be discussed in detail in Section V-B below.

V. DISCUSSION AND CONCLUSIONS

A. Pressure Waves p_1' and p_2' Produced by a Heater

In the measurements of the pressure wave amplitudes p_1' and p_2' produced by a heater the temperature dependence of p_1' was in good agreement with the theoretical expression of Eq. 63. However, these experimental results indicate that there are contributions to p_2' in addition to that obtained by merely retaining the thermal expansion coefficient in the two-fluid hydrodynamic equations. Recall that the theoretical expressions, Eqs. 63 and 65, were obtained from the set of hydrodynamic equations, 8-11, in which no dissipative terms were included. The effect of retaining some of these dissipative terms will now be examined.

Dingle,[39] using the method of Lifshitz,[6] has calculated the coupling coefficients when terms due to the viscosity η of the normal fluid are included in the hydrodynamic equations. He took into account both the viscous forces in the bulk liquid and also the forces at the walls when the liquid is confined in a cylindrical tube. The resulting contribution to the coupling coefficients due to the viscous forces in the bulk liquid is negligibly small compared to that due to α. This is also true for

the contribution due to the viscous forces at the tube walls, except for p_2' waves at low frequencies and temperatures below about 1.4 K.

We have extended the calculations by also including in the hydrodynamic equations terms due to the coefficient of second viscosity ζ_2 and the thermal conductivity coefficient κ. The coefficient of second viscosity is an order of magnitude larger than the normal fluid viscosity η and contributes the largest term in the expression for the attenuation of first sound.[5] The attenuation of second sound is due mainly to the thermal conductivity coefficient.[5]

The results of these calculations are that the contribution to the coupling due to the thermal conductivity coefficient is negligibly small compared to that of α. This is true for both p_1' and p_2' waves at all temperatures in the range of our investigations. The combined contribution of η and ζ_2 is also negligibly small compared to that of α, except for p_2' waves at temperatures below about 1.4 K.

When η and ζ_2 are retained in the hydrodynamic equations 1-4 and the viscous forces at the walls of the tube are taken into account, Eqs. 63 and 64 for the pressure wave amplitudes p_1' and p_2' produced in liquid helium by a fluctuating temperature source take the following form:

$$p_1' = \left\{\alpha + \frac{C}{ST}\left(\frac{u_2}{u_1}\right)^2\left[\left(\frac{4}{3}\eta + \zeta_2\right)\left(\frac{1\omega}{\rho u_1^2}\right) + \frac{2(1+1)}{\rho r}\left(\frac{\eta\rho_n}{2\omega}\right)^{\frac{1}{2}}\right]\right\}\rho u_1 u_2 T_o \quad (99)$$

$$p_2' = -\left\{\alpha + \frac{C}{ST}\left[\left(\frac{4}{3}\eta + \zeta_2\right)\left(\frac{1\omega}{\rho u_2^2}\right) + \frac{2(1+1)}{\rho r}\left(\frac{\eta\rho_n}{2\omega}\right)^{\frac{1}{2}}\right]\right\}\rho u_2^2 T_o \quad . \quad (100)$$

In Eqs. 99 and 100, r is the radius of the cylindrical chamber. These results were obtained from the hydrodynamic equations by the same procedure as was used in Section II to obtain Eqs. 63 and 64.

Both terms which are added to α in Eq. 99 are negligibly small compared to α. However in Eq. 100 the first term, $(C1\omega/ST\rho u_2^2)(4\eta/3 + \zeta_2)$, is the same order of magnitude as α for temperatures below about 1.4 K and at the higher frequency of 10 kHz used in the pulse measurements. Similarly the second term, $\left(2C(1+1)/ST\rho r\right)\left(\eta\rho_n/2\omega\right)^{\frac{1}{2}}$, is the same order of magnitude as α below about 1.4 K and at the low frequencies used in the standing wave measurements.

The correction due to the first term at a frequency of 10 kHz is represented on Figure 16 by the dashed line. The correction due to the second term is about the same order of magnitude at frequencies in the range from 75 Hz to 190 Hz and has thus not been shown on this figure.

The combined effect of η and ζ_2 does therefore provide a mechanism which results in the production, by a fluctuating temperature source, of larger amplitude p_2' waves while not affecting the p_1' amplitude. This

contribution increases with decreasing temperature and is not zero at the temperature where α vanishes. Thus the corrections due to this mechanism do shift the theoretical curves in the right direction; that is, toward better agreement with the experimental data. However, as can be seen in Figure 16, the magnitude of these corrections is still much too small to bring about good agreement between the experimental p_2' data and the theory.

The values of η used in the above analysis were those measured by Tough et al.[40] and the values of ζ_2 were those calculated by Khalatnikov and Chernikova.[41]

Hofmann et al.[9] have also observed a larger amplitude p_2 wave produced by a heater than predicted by the theory based on the two-fluid hydrodynamic equations with α retained. They suggest that this might be due to the microphone receiver being more sensitive to p_2' pressure waves than to p_1' pressure waves. This appears unlikely since both waves were propagated at the same frequency. The microphone sensitivity would therefore depend upon wavelength. We have not been able to devise a technique whereby this speculation might be checked.

3. Temperature Wave T_2' Produced by a Microphone

There are a number of factors which might explain the discrepancy between the experimental T_2' data and the theoretical curve on Figure 18. We have found that the contributions to T_2' due to the normal fluid viscosity and the coefficient of second viscosity in the bulk liquid

are negligible. However, the correction, calculated by Dingle,[39] due to the viscous forces at the walls of the chamber should be considered. When this is done, the expression for the temperature wave amplitude T_2' produced by a vibrating diaphragm (see Eq. 54) takes the following form:

$$T_2' = \left[\alpha - \frac{2C(1+1)}{sT\rho r}\left(\frac{\eta\rho_n}{2\omega}\right)^{\frac{1}{2}}\right]\frac{Tu_2}{C}u_o \quad . \qquad (101)$$

In Figure 18 the solid line is the theoretical curve of $T_2'/u_o = \alpha Tu_2/C$ from Eq. 54 while the dashed line is that of Eq. 101. As can be seen, the correction, although not negligible, is much too small to explain the discrepancy.

Another possible source of the discrepancy is the fact that it has been assumed that the velocity amplitude u_o of the transmitter diaphragm is constant. This may not be the case. As previously indicated, for a driving force $F = F_o\exp(i\omega t)$, the velocity amplitude of the diaphragm will be[24]:

$$u_o = \frac{F_o}{Z_m + Z_r} \qquad (102)$$

In Eq. 102, Z_m is the mechanical impedance of the diaphragm and Z_r is the acoustic radiation impedance of the liquid helium.

The mechanical impedance of the diaphragm is given by[4]:

$$Z_m = R + i\left(\omega M - \frac{S}{\omega}\right) = R + i\omega M\left[1 - \left(\frac{\omega_o}{\omega}\right)^2\right], \quad (103)$$

where M is the mass of the diaphragm, S is the stiffness, R is the mechanical resistance which results in dissipation, and $\omega_o^2 = S/M$. The radiation impedance is proportional to ρu_1.

The quantity ρu_1 is not strongly temperature dependent. It increases monotonically from T = 1.2 K to T_λ with the total variation being about 8%. Thus if $Z_r \gg Z_m$, the velocity amplitude of Eq. 102 would vary little with temperature.

We do not have quantitative knowledge of the parameters of the microphone. Thus the relative amplitudes of Z_m and Z_r cannot be calculated. However some qualitative arguments can be made which would indicate that the variation of Z_m in this experiment is also small. Investigations by Bell, et al.[40] of the properties of capacitor microphones similar to the ones used in these investigations indicate that the resonant frequency, ω_o, was 10 - 15 kHz or higher. The frequencies used in the standing wave measurements of T_2' were in the range from 75 Hz to 190 Hz. It is therefore probably safe to assume that $\omega \ll \omega_o$ in these measurements. At frequencies far from resonance it is often usually possible to neglect the mechanical resistance, R.[24]

In this case Eq. 103 gives $Z_m \cong iM\omega_o^2/\omega$. If it is also assumed that $Z_m \gg Z_r$ then, from Eq. 102, u_o would be proportional to ω. However, the resulting correction to the T_2' data due to the variation of frequency in the standing wave measurements is still much too small to substantially reduce the discrepancy between the data and theory.

A final consideration which might be the cause of the discrepancy between the T_2' data and the theoretical expression of Eq. 54 is the fact that the porous diaphragm transducer will also be sensitive to pressure waves. This was already mentioned in Section IV-B-2 where it was pointed out that resonances of waves propagating at u_1 were also observed in this experiment. The question is: Are these resonances of p_1' of Eq. 51 or of T_1' of Eq. 52 or both? Actually a better way to put the question is: What is the relative sensitivity of the porous diaphragm transducer to pressure and temperature waves?

The same question is involved in the observation of resonances corresponding to waves propagating at u_2. Could there be a significant contribution to the received signal due to the p_2' waves of Eq. 53? Since α is very small, Eqs. 53 and 54 would indicate that p_2', which is proportional to α^2, could be neglected in comparison to T_2', which is proportional to α. However this may not be true if the porous diaphragm transducer is more sensitive to pressure waves than to temperature waves.

We have not been able to arrive at a definite quantitative answer to these questions. However, certain results obtained in our investigations and also the results of the investigation by Sherlock and Edwards[21] would seem to indicate that the porous diaphragm transducer is a more efficient receiver of temperature waves than of pressure waves.

Recall the following two experiments which were performed in this investigation. First a regular capacitor microphone was used as the receiver in the experiment in which the transmitter was a periodically heated carbon disk resistor. In this case two pressure waves, one propagating at u_1 and the other at u_2, were observed. In a succeeding experiment, described in Section IV-B-1, the same carbon disk transmitter was used but the receiver was now the porous diaphragm transducer. In this case only waves propagating at u_2 were observed. Moreover the output signal from this wave was two orders of magnitude larger than that from the u_2 wave in the first experiment.

In the first experiment the two waves were p_1' and p_2' of Eqs. 63 and 65 because the regular capacitor microphone is sensitive only to pressure waves. In the second experiment the received signal could be due to either p_2' or T_2' of Eqs. 65 and 66 respectively. However, if the contribution of p_2' to this signal were significant, then we should also have been able to observe p_1' waves in this experiment.

The fact that we did not observe any waves propagating at u_1 in the second experiment, but did observe very strong signals corresponding to waves propagating at u_2, would indicate that the porous diaphragm transducer is a more efficient receiver of temperature waves than of pressure waves. This conclusion is also indicated from the work of Sherlock and Edwards.[21] They used a configuration in which both transmitter and receiver were porous diaphragm transducers. They also observed only waves propagating at u_2.

These results indicate that the discrepancy between the T_2' data and the theoretical expression of Eq. 54 is not due to a contribution from p_2' of Eq. 53. However it is still not clear what the relative contributions of p_1' and T_1' of Eqs. 51 and 52 are to the u_1 resonances which were observed. In this case T_1' is proportional to α while p_1' is not. Thus these resonances could still be due mainly to p_1'. The fact that the amplitude of these resonances varied little with temperature would seem to indicate that this is the case since ρu_1 in Eq. 51 is relatively independent of temperature compared to the corresponding coefficient in Eq. 52.

A qualitative study of these u_1 resonances was hindered by the same problems (see Section III-A-2) which prevented the use of the standing wave technique to study the p_1' waves produced by a heater. The exact nature of

the u_1 waves in this experiment might be better understood if they could be observed and studied with pulses.

LIST OF REFERENCES

LIST OF REFERENCES

1. J. Wilks, The Properties of Liquid and Solid Helium, (Clarendon Press, Oxford, 1967).

2. W. E. Keller, Helium-3 and Helium-4, (Plenum Press, New York, 1969).

3. R. P. Feynman, in Progress in Low Temperature Physics, edited by C. J. Gorter (North Holland Publishing Company, Amsterdam, 1957), Vol. I, pp. 17-53.

4. L. Landau, J. Phys. Moscow 5, 71 (1941).

5. I. M. Khalatnikov, An Introduction to the Theory of Superfluidity, (W. A. Benjamin, Inc., New York, 1965).

6. E. Lifshitz, J. Phys. Moscow 8, 110 (1944).

7. G. Jacucci and G. Signorelli, Phys. Letters 26A, 5, (1967).

8. G. V. Eynatten, W. Veith, and F. Pobell, Unpublished private communication.

9. A. Hofmann, K. Keck, and G. U. Schubert, Z. Physik 231, 177 (1970).

10. V. P. Peshkov, J. Phys. Moscow 10, 389 (1946). The work of Shalnikov and Sokolov is mentioned in this paper.

11. C. C. Lin, in Liquid Helium, edited by G. Careri (Academic Press, New York, 1963). p. 93

12. A. Sommerfeld, Lectures on Theoretical Physics, Vol. V - Thermodynamics and Statistical Mechanics, (Academic Press, New York, 1964).

13. C. T. Lane, Superfluid Physics, (McGraw-Hill, New York, 1962).

14. L. D. Landau and E. M. Lifshitz, Course of Theoretical Physics, Vol. 6 - Fluid Mechanics, (Addison-Wesley Publishing Co., Inc., Reading Mass., 1959).

15. I R C Inc., Boone Division, Boone, N. C. 28607

16. Amphenol Type RG - 174/V

17. Norton Co., Metallized Products Division, Winchester, Mass. 01890.

18. F. E. Hoare, L. C. Jackson, and N. Kurti, Experimental Cryophysics, (Butterworth and Co., London, 1961).

19. L. Beranek, Acoustics, (McGraw-Hill Book Co., New York, 1954), p. 292.

20. Millipore Corp. Bedford, Mass. 01730

21. R. A. Sherlock and D. O. Edwards, (To be published).

22. R. Williams, E. A. Beaver, J. C. Fraser, R. S. Kagiwada, and I. Rudnick, Phys. Letters 29A, 279 (1969).

23. R. A. Sherlock, N. R. Brubaker, D. O. Edwards, R. E. Sarwinski, and P. F. Seligmann, Bull. Am. Phys. Soc. 15, 58 (1970).

24. L. E. Kinsler and A. R. Frey, Fundamentals of Acoustics, (J. Wiley and Sons, Inc., New York, 1950) p. 80.

25. K. R. Atkins and K. H. Hart, Phys. Rev. 92, 204 (1953).

26. W. B. Hanson and J. R. Pellam, Phys. Rev. 95, 321 (1954).

27. K. N. Zinov'eva, Zh. eskp. teor. Fiz. 31, 31 (1956); Soviet Phys. JETP 4, 36 (1957).

28. E. C. Kerr and R. D. Taylor, Ann. Phys. 26, 292 (1964)

29. H. C. Kramers, J. D. Wasscher, and C. J. Gorter, Physica 18, 329 (1952).

30. R. W. Hill and O. V. Lounasmaa, Phil. Mag. 2, 143 (1957).

31. R. D. Maurer and M. A. Herlin, Phys. Rev. 76, 948 (1949)

32. J. R. Pellam, Phys. Rev. 75, 1183 (1949)

33. V. P. Peshkov, Zh. eksp. teor. Fiz. 38, 799 (1960); Soviet Phys. JETP 11, 580 (1960).

34. P. de Lange, Proc. Roy. Soc. 91, 239 (1915).

35. H. D. Arnold and I. B. Crandall, Phys. Rev. 10, 22 (1917).

36. E. C. Wente, Phys. Rev. 19, 333 (1922).

37. S. Ballantine, J. Acous. Soc. Am. 3, 319 (1932).

38. H. A. Fairbank, W. M. Fairbank, and C. T. Lane, J. Acous. Soc. Am. 19, 475 (1947).

39. R. B. Dingle, Proc. Phys. Soc. London 63A, 638 (1950).

40. J. T. Tough, W. D. McCormick, and J. G. Dash, Phys. Rev. 132, 2373 (1963).

41. I. M. Khalatnikov and D. M. Chernikova, Soviet Phys. JETP 23, 274 (1966).

42. W. Kuhl, G. R. Schodder, and F. K. Schroder, Acoustica 4, 519 (1954).